



Decoding the origins and sources of clay minerals in the Upper Cretaceous Tununk Shale of south-central Utah: Implications for the pursuit of climate and burial histories

Zhiyang Li | Juergen Schieber | David Bish

Department of Earth and Atmospheric Sciences, Indiana University, Bloomington, IN, USA

Correspondence

Zhiyang Li, Indiana University Department of Earth and Atmospheric Sciences, Bloomington, IN, USA.
Email: zl29@iu.edu

Funding information

American Association of Petroleum Geologists; Geological Society of America; Society for Sedimentary Geology

Abstract

Clay minerals in fine-grained marine sedimentary successions are most commonly considered to be detrital in origin and have been used extensively by geologists as indicators of palaeoclimate conditions in the hinterland. Most of these previous studies, however, were not designed to address in depth the potential effects of mixing clay minerals from multiple sources and the formation of authigenic clay minerals during early diagenesis on the ultimately observed clay mineral assemblages of fine-grained marine sedimentary successions. Herein, clay minerals in shales and bentonites of the Tununk Shale Member in south-central Utah were examined through integrated X-ray diffraction and petrographic (scanning electron microscopy) analysis, to evaluate the various origins of clay minerals in this offshore mudstone succession. Clays in Tununk bentonites contain dominantly smectite (>80%) and a minor amount of kaolinite. Clays in Tununk shale samples consist dominantly of mixed-layer illite/smectite with up to 45% illite-like layers, small amounts of kaolinite and mica, and in places trace amounts of chlorite. Clay minerals in Tununk shale samples occur in the following three forms: (a) in clay-dominated aggregates (i.e. smectite-dominated altered volcanic rock fragments and illite/smectite-dominated shale lithics); (b) in the fine-grained matrix (mostly illite/smectite and minor amounts of mica and kaolinite); and (c) in intergranular and intragranular pore spaces (authigenic smectite, kaolinite and chlorite). Possible sources for the mixed-layer illite/smectite in shales include (a) erosion of older smectite-bearing mudstone successions and (b) weathering of volcanic rocks or volcanic debris that had been deposited on land. Most of the kaolinite and chlorite in the Tununk Shale were precipitated as pore-filling cements, rather than having a terrigenous source (as weathering products). A comprehensive understanding of the multiple origins of clay minerals (e.g. terrigenous input, volcanic input, recycled sediments and diagenesis) in marine mudstone successions is critical when attempting to use clay mineral data for reconstructions of palaeoclimate and burial and thermal histories.

KEY WORDS

Clay mineralogy, mudstone petrography, mudstone provenance, palaeoclimate, recycled sediments, volcanic ash

1 | INTRODUCTION

Clay minerals dominate the clay-sized fraction ($< 4 \mu\text{m}$) of many fine-grained sedimentary (mudstone/shale) successions (Chamley, 1989; Velde, 1995; Potter *et al.*, 2005; Lazar *et al.*, 2015). Particularly in marine strata, clay mineral assemblages have been widely used as a palaeoclimate proxy (Singer, 1980, 1984; Curtis, 1990; Robert and Kennett, 1997; Tamburini *et al.*, 2003; Colin *et al.*, 2014; Wendler *et al.*, 2016). This is because clay minerals in marine sediments were generally assumed to be inherited from landmasses via weathering of bedrock, which is ultimately controlled by climate (Biscaye, 1965; Chamley, 1989; Hallam *et al.*, 1991; Junntila *et al.*, 2005; Dera *et al.*, 2009; Liu *et al.*, 2010; Wendler *et al.*, 2016). The other underlying assumption for using clays as palaeoclimate proxies is that sedimentary clay mineral assemblages have not been altered significantly by diagenetic processes (Singer, 1984; Curtis, 1990; Ruffel *et al.*, 2002; Kemp *et al.*, 2016; Xu *et al.*, 2017).

Recent advances in the understanding of the provenance and depositional processes of fine-grained sediments, however, indicate that clay minerals in mudstones can have a wide variety of origins. The complex sources and dispersal processes (and pathways) of fine-grained sediments in marine environments, as revealed by sedimentologic and petrographic analysis (Macquaker *et al.*, 2014; Taylor and Macquaker, 2014; Harazim and McIlroy, 2015; Lazar *et al.*, 2015; Li *et al.*, 2015; Wilson and Schieber, 2015; Schieber, 2016a; Li and Schieber, 2018a; DeReuil and Birgenheier, 2019), pose challenges for the interpretation of climate signals from clay mineral assemblages of ancient marine mudstone successions (Clayton *et al.*, 1999; Thiry, 2000). The common occurrence of silt to sand-sized clay-dominated composite particles (aggregates) of multiple origins in both ancient and modern fine-grained deposits (Macquaker *et al.*, 2010; Plint *et al.*, 2012; Schieber, 2016b; Laycock *et al.*, 2017; Shchepetkina *et al.*, 2018; Li and Schieber, 2018b) strongly suggests that the origin of clay minerals in fine-grained sedimentary successions is a much more complex issue than commonly presumed.

In addition, there has been comparatively little consideration of authigenic clays formed during early diagenesis (within the first few metres of burial) and their contribution to the observed clay mineral assemblages in mudstones, although the formation of authigenic clays as well as the transformation of specific clay types (e.g. smectite to illite) during deep burial has been studied extensively (Burst, 1957; Nadeau and Reynolds, 1981a; Sucha *et al.*, 1993; Hillier *et*

al., 1995; Anjos *et al.*, 2003). Early diagenetic processes in mudstones are largely driven by redox reactions, in which sedimentary organic matter is metabolized by microbes (Froelich *et al.*, 1979; Wilson *et al.*, 1985; Canfield *et al.*, 1993; Chester, 2009). Key products of these reactions include bicarbonate ions, reduced manganese and iron, and sulphide, all of which can be incorporated into early diagenetic minerals such as calcite, pyrite, siderite and dolomite (Berner, 1984; Raiswell, 1988; Macaulay *et al.*, 1993; Raiswell and Fisher, 2000; Taylor *et al.*, 2000). That clay minerals can also form during this shallow burial stage has been known for some time (Odin, 1990; Mackenzie and Kump, 1995; Michalopoulos and Aller, 1995) but still is not considered of significant importance in many published studies of mudstones. Over the past decade, an increasing number of case studies have suggested that significant amounts of kaolinite in some ancient mudstone successions is of early diagenetic origin (Aplin and Macquaker, 2012; Macquaker *et al.*, 2014; Taylor and Macquaker, 2014; Schieber *et al.*, 2016), instead of being introduced to sedimentary basins by rivers that had intensely weathered soils in their catchment areas (Thiry, 2000; Junntila *et al.*, 2005; Wendler *et al.*, 2016).

Presumed Milankovitch-scale climate cycles during the Late Cretaceous have been widely reported (Barron *et al.*, 1985; Sageman *et al.*, 1997; Floegel *et al.*, 2005; Eldrett *et al.*, 2015; Wendler *et al.*, 2016). Many of these studies focusing on Late Cretaceous strata in the Western Interior Seaway (WIS) of North America interpreted variations in the relative amount of clay minerals of presumed detrital origin as high-frequency wet versus dry cycles (Pratt, 1984; Eicher and Diner, 1989; Sethi and Leithold, 1994). In the pelagic deposits of the Bridge Creek Limestone Member that accumulated in the central area of the WIS (at Pueblo, Colorado; Figure 1A), discrete illite and mixed-layer illite/smectite (I/S) are considered of detrital and volcanic origin, respectively (Pratt, 1984; Eicher and Diner, 1989). However, analysis of the clay mineralogy in proximal time-equivalents of the Bridge Creek Limestone, the Tropic Shale and Tununk Shale in southern Utah along the western margin of the WIS (Figure 1A), shows a much more complex assemblage of presumed detrital clays, including kaolinite, discrete illite, chlorite, and mixed-layer I/S (Sethi and Leithold, 1994). The discrepancies in the presumed detrital clay mineral assemblages suggested by these studies highlight the inherent difficulties in resolving the complex origins of clay minerals in marine sedimentary successions. These issues severely limit our ability to untangle clay mineral signals that reflect climate changes from those

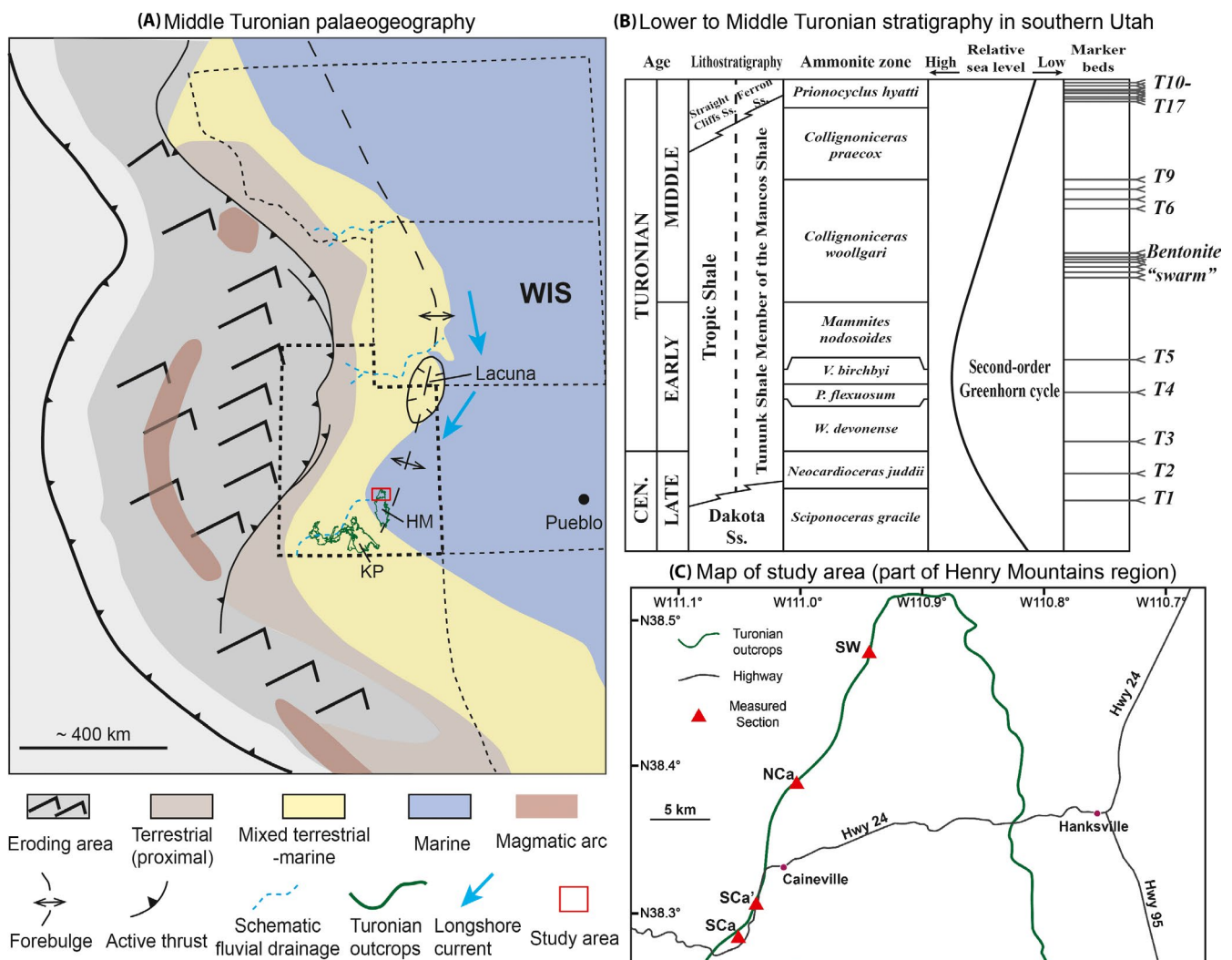


FIGURE 1 A) Palaeogeographic reconstruction of the foreland basin of middle North America that shows evolving topography (schematic), locations of active faults, general depositional environments and forebulge position during the Turonian (modified from Yonkee and Weil, 2015). WIS: Western Interior Seaway. The lacuna in north-eastern Utah developed as a submarine unconformity from the late Cenomanian to middle Turonian due to the uplift of an intrabasinal culmination (Ryer and Lovekin, 1986). Outcrops of the Tununk Shale and Tropic Shale are distributed in the Henry Mountains Region (HM) and Kaiparowits Plateau (KP), respectively. B) Lower to middle Turonian stratigraphy in Southern Utah (compiled from Kauffman, 1977; Zelt, 1985; Leithold, 1994; Leithold and Dean, 1998). C) Map of study area in the Henry Mountains region. The location of C) is indicated by the red box in A). Red triangles indicate locations of three measured stratigraphic sections (SW: Salt Wash, NCa: North Caineville, and SCa: South Caineville). The section measured at SCa is a composite section consisting of two segments (SCa and SCa').

due to changes in depositional environment, provenance and diagenesis.

Most previous palaeoclimate interpretations in mudstones were based on the clay mineral assemblages determined via X-ray diffraction (XRD) methods (Moore and Reynolds, 1997). Yet, without detailed petrographic (scanning electron microscope) examination of the morphology, texture and distribution of clay minerals in fine-grained sedimentary successions, the exact origin of clay minerals and the impact of early diagenesis cannot be evaluated with confidence. This study focusses on the Upper Cretaceous Tununk Shale Member of the Mancos Shale in south-central Utah because the presumption is that it should carry a clearer and stronger

detrital clay signal due to its proximal setting within the WIS. The Tununk Shale in the study area has undergone negligible burial metamorphism (Nadeau and Reynolds, 1981a), making it an ideal natural laboratory for constraining detrital clay inputs to the WIS. Based on integrated X-ray diffraction and petrographic (scanning electron microscopy) analysis, clay minerals in the Tununk Shale can be traced to multiple sources (e.g. wind-borne volcanic ash, recycled sediments and diagenesis) in addition to continental weathering. It is therefore critical to obtain a comprehensive understanding of the sources and origins of clay minerals in marine mudstone successions before using clay mineral assemblages as proxies for palaeoclimate conditions and burial and thermal histories.

2 | GEOLOGICAL BACKGROUND

During the Late Jurassic and Cretaceous, the geology of western North America was largely controlled by the subduction of the Farallon plate beneath the North American plate (Livaccari, 1991; DeCelles, 2004). The compressive forces associated with plate convergence, combined with conductive heating initiated by subduction, led to crustal thickening in orogenic belts such as the Sevier fold-thrust belt (Livaccari, 1991; DeCelles, 2004). Subsidence due to flexural loading of the crust formed an asymmetric foreland basin, bounded to the west by the rising Sevier orogenic belt and to the east by the stable North American craton (Kauffman, 1977, 1985; Kauffman and Caldwell, 1993). During the Late Cretaceous, the foreland basin was subject to active thrusting, subsidence, uplift (forebulge uplift) and extensive volcanism (DeCelles, 2004; DeCelles and Coogan, 2006; Yonkee and Weil, 2015). A magmatic arc, comprising a belt of calc-alkaline intrusive and volcanic rocks, was located along the western margin of the North American continent (Figure 1A).

The combined effects of load-induced subsidence and eustatic highstand throughout the Late Cretaceous resulted in the development of an epicontinental seaway known as the WIS (Kauffman, 1977, 1985). During the Albian to Maastrichtian, the WIS was subject to five major transgressive-regressive marine cycles with durations of 2–10 Myr (Kauffman, 1985). The most extensive flooding of the seaway occurred during the so-called Greenhorn cycle, when more than one-third of North America was inundated. The Greenhorn cycle began in the late Albian and ended in the middle Turonian (Kauffman, 1985). During peak transgression in the early Turonian, the WIS extended from the Arctic Ocean to the present-day location of the Gulf of Mexico and was characterized by a broad shelf (Figure 1A). In response to sediments supplied from the unroofing of the Sevier orogenic belt and volcanic highlands to the west, the WIS was characterized by high siliciclastic input and high sedimentation rates along its western margin (Kauffman, 1977, 1985).

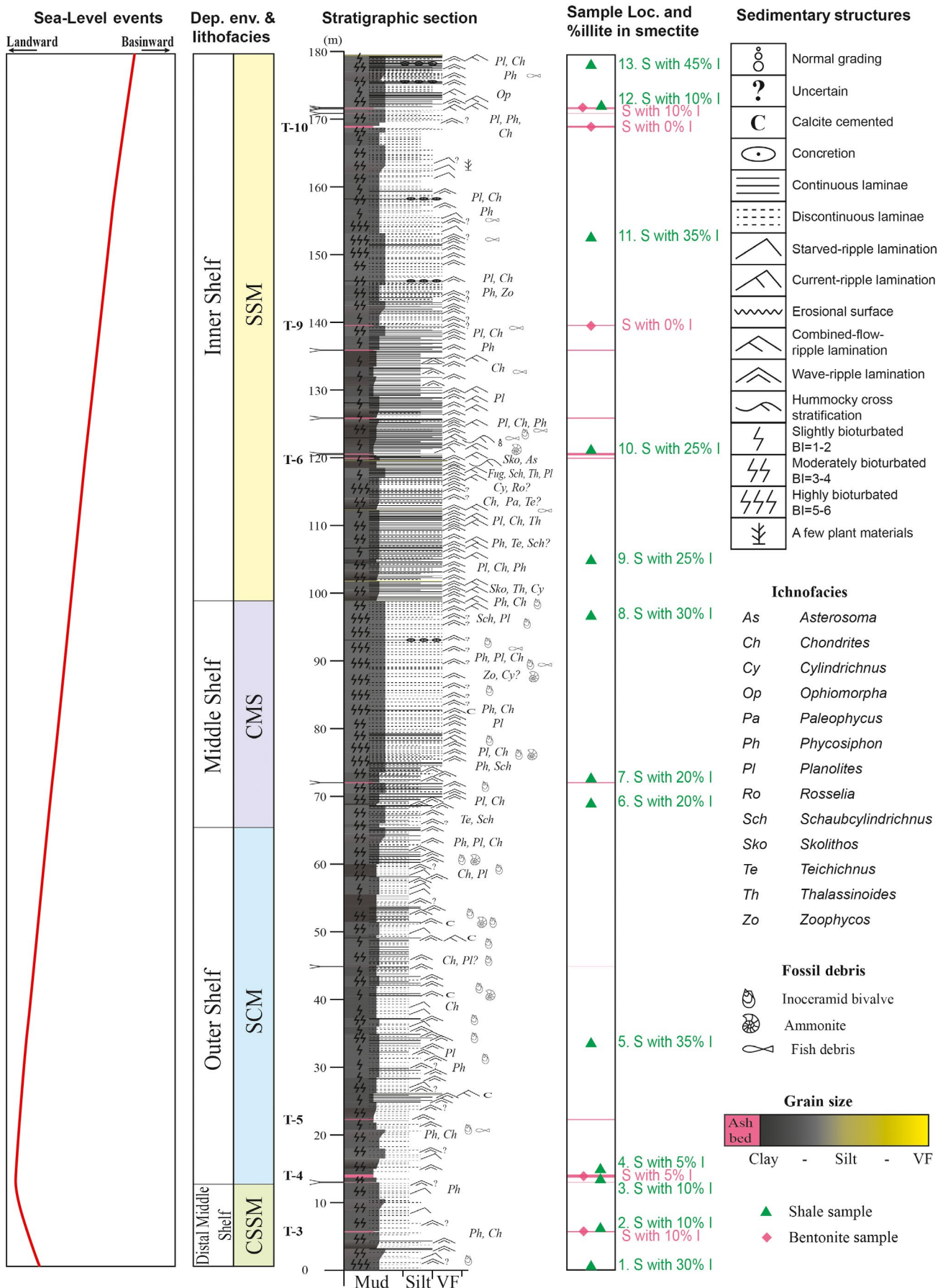
The Tununk Shale accumulated along the western margin of the WIS during the late Cenomanian to middle Turonian. In outcrop it consists mainly of dark grey calcareous to non-calcareous mudstones with numerous thin silt and sand-rich beds (Peterson *et al.*, 1980; Zelt, 1985). A series of

regionally traceable bentonite beds has been used to correlate the Tununk Shale in south-central Utah (Henry Mountains Region) with its lateral equivalent, the Tropic Shale in southern Utah (Kaiparowits Plateau) (Zelt, 1985; Leithold, 1994; Figure 1). Driven by the Greenhorn transgressive-regressive sea-level cycle, the offshore mudstones of the Tununk Shale overlie the coarser non-marine and paralic deposits of the Dakota Sandstone and grade upward into the shallow marine and deltaic strata of the Ferron Sandstone Member (Figure 1B). The palaeoshoreline during deposition of the Tununk Shale generally trended north-east–south-west (Figure 1A; Zelt, 1985; Leithold, 1994). Although the dominant direction of sediment progradation was eastwards, nearshore sediments deposited along the western margin of the WIS were deflected southwards by coastal currents generated by a large-scale counterclockwise gyre (Figure 1A; Barron, 1989; Erickson and Slingerland, 1990; Slingerland and Keen, 1999; Li *et al.*, 2015).

2.1 | Depositional framework of the Tununk Shale

Characteristics of sedimentary facies and depositional framework of the Tununk Shale are discussed in detail in a previous study (Li and Schieber, 2018a), and are only briefly summarized here. The Tununk Shale in the study area is interpreted as an offshore mud belt on a storm-dominated shelf and consists of four shale lithofacies associations. In detail these are: (a) carbonate-bearing (<30% carbonate), silty and sandy mudstone (CSSM); (b) silt-bearing, calcareous mudstone (SCM, >30% carbonate); (c) carbonate-bearing, silty mudstone to muddy siltstone (CMS); and (d) non-calcareous, silty and sandy mudstone (SSM) (Figure 2), based mainly on the relative proportion of carbonate particles derived from carbonate productivity versus siliciclastic particles of detrital origin. A series of bentonite beds are present throughout the Tununk Shale (Figures 1B and 2). Upsection, the relative amount of the carbonate component derived from carbonate productivity gradually increases from the CSSM to SCM, then decreases to the CMS, and was not observed in the SSM lithofacies association. Vertical variations in lithofacies association and sedimentary facies characteristics indicate that the depositional environment of the Tununk Shale shifted laterally from distal middle-shelf to outer-shelf

FIGURE 2 A representative stratigraphic section of the Tununk Shale measured at North Caineville (NCa), with the second-order Greenhorn sea-level cycle, general lithofacies packages and interpreted depositional environments. The stratigraphic locations of both shale and bentonite samples for XRD analysis in this study and the relative amount of illite-type layer in the mixed-layer I/S (0% I indicates pure smectite) are presented. T3–T10 represent regionally continuous bentonite marker beds after Zelt (1985). The Tununk Shale consists of a stack of four lithofacies associations including: 1) carbonate-bearing, silty and sandy mudstone (CSSM), 2) silt-bearing, calcareous mudstone (SCM), 3) carbonate-bearing, silty mudstone to muddy siltstone (CMS), and 4) non-calcareous, silty and sandy mudstone (SSM). The same facies characteristics and lithofacies stacking patterns are also observed in the other two measured sections (Li and Schieber, 2018a)



(CSSM to SCM), then from outer-shelf to inner-shelf environment (SCM to CMS, and to SSM) during the second-order Greenhorn sea-level cycle (Figure 2). Storm-induced, shore-parallel geostrophic flow and offshore-directed flows probably were the dominant processes that governed the transport and deposition of mud along and across a storm-dominated shelf (Li and Schieber, 2018a).

3 | METHODS

Samples (shales and bentonites) for this study were collected from three detailed stratigraphic sections of the Tununk Shale near Hanksville, Utah (Figures 1C and 2). By comparing the composition and characteristics of clay minerals of bentonites with those of shale samples, the sources (other than volcanic ash) of clay minerals in Tununk shale samples can be determined. Forty-two representative shale samples and five bentonite samples from all lithofacies associations throughout the Tununk Shale were selected to make polished thin sections and ion-milled samples (up to 12 mm in diameter) for subsequent scanning electron microscopy (SEM) analysis. Detailed petrographic examination was conducted to determine the overall composition, as well as the type, morphology, texture and distribution of clay minerals present in both shales and bentonites using an FEI Quanta 400 scanning electron microscope, operating at 15 kV and a working distance of 10 mm. Energy-dispersive X-ray spectroscopy (EDS) was used to aid determination of mineralogy.

Five samples of bentonites and 13 samples of shales (including those next to and farther away from bentonites) throughout measured section NCa (Figure 1C) were selected for determination of clay mineral assemblages in the $<2\text{ }\mu\text{m}$ fractions by XRD analysis. The stratigraphic locations of these samples are indicated in Figure 2. Samples were crushed and dispersed in distilled water using an ultrasonic probe. For each sample, the $<2\text{ }\mu\text{m}$ fraction was separated by gravity settling in water, concentrated by centrifugation and prepared for XRD analysis by sedimentation onto a quartz plate ('zero-background' plate). The XRD patterns were acquired using a Bruker D8 Advance X-ray diffractometer equipped with incident and diffracted-beam Soller slits, a Sol-X solid-state Si (Li) energy-dispersive detector and CuK α radiation (45 kV, 35 mA). The $<2\text{ }\mu\text{m}$ fraction was scanned from 2 to $36^\circ 2\theta$ in the air-dried state and after saturation with ethylene glycol. Estimates of the percentage of illite-type layers (collapsed layers) in the mixed-layer I/S were made based on the peak positions of glycolated mixed-layer I/S from about 26° to $27^\circ 2\theta$ and from 15.4° to $17.7^\circ 2\theta$, using the method described by Šrodoň (1980). The accuracy of the determination of the percentage of expandable layers was $\pm 5\%$ for most mixed-layer I/S samples (Šrodoň, 1980).

4 | CLAY MINERALOGY OF THE TUNUNK SHALE

4.1 | Clay minerals in bentonites

Bentonite beds in the Tununk Shale range from 1 to 40 cm in thickness (Figure 2). On polished slabs, some bentonite beds are slightly to moderately bioturbated (Figure 3A and B) and show navichnia traces (sediment-swimmer traces sensu Lobza and Schieber, 1999). On polished slabs, bentonites can be structureless or show a variety of sedimentary structures such as ripple-scale cross lamination, stacked normally graded beds, and erosional bases (Figure 4). The $<2\text{ }\mu\text{m}$ fractions of bentonites consist almost exclusively of smectite or mixed-layer I/S with up to 10% illite-type layers (Figures 2 and 4). In a few bentonite samples, a small peak near 7.0 \AA indicates the presence of a small amount of kaolinite (Figure 4).

Under the SEM, un-reworked ash-fall bentonites (those showing no features indicating reworking by bioturbation or bottom currents) in the Tununk Shale contain common silt to sand-sized phenocrysts, including biotite, plagioclase, potassium-feldspar and small amounts of apatite and quartz (Figure 5A and B). The clay mineral-dominated matrix of un-reworked bentonites consists exclusively of smectite, characterized by a highly crenulated and honeycombed morphology (Figure 5C). The small amount of kaolinite present in some bentonites is mostly associated with biotite (Figure 5B and D).

4.2 | Clay minerals in shales

The $<2\text{ }\mu\text{m}$ fractions of shale samples show a more complex composition. The sharp peaks at 26.6° and 29.4° are due to the presence of micron-sized quartz and calcite (as coccolith debris), respectively (Figure 6). The relative intensity of the quartz and calcite peaks is consistent with different lithofacies associations having varying carbonate content in the Tununk Shale. The dominant type of clay mineral in the shale samples is mixed-layer I/S with varying proportions of illite-type layers. Compared with the bentonites, the $<2\text{ }\mu\text{m}$ fractions of shales contain greater amounts of mica and kaolinite (Figure 6B), indicated by peaks at $\sim 10.0\text{ \AA}$ and 7.0 \AA , respectively. The partial resolution of two peaks at $\sim 7.0\text{ \AA}$ and 3.5 \AA in a few samples indicates the presence of trace amounts of chlorite (Figure 6B). The mixed-layer I/S in shales close to bentonites contains 5%-10% illite-type mixed layers (Figures 6A and 7). In shales far ($>1\text{ m}$) away from bentonite beds, the 001 peak of the mixed-layer I/S shows significant broadening (Figure 6B). In these shale samples, a distinctly higher amount (20%-45%) of illite-type layers is present in the mixed-layer I/S (Figures 2 and 6B).

Detailed SEM examinations indicate that clay minerals in shale samples are present in three forms: (a) as clay-dominated composite particles (or aggregates) (Figure 8); (b) in

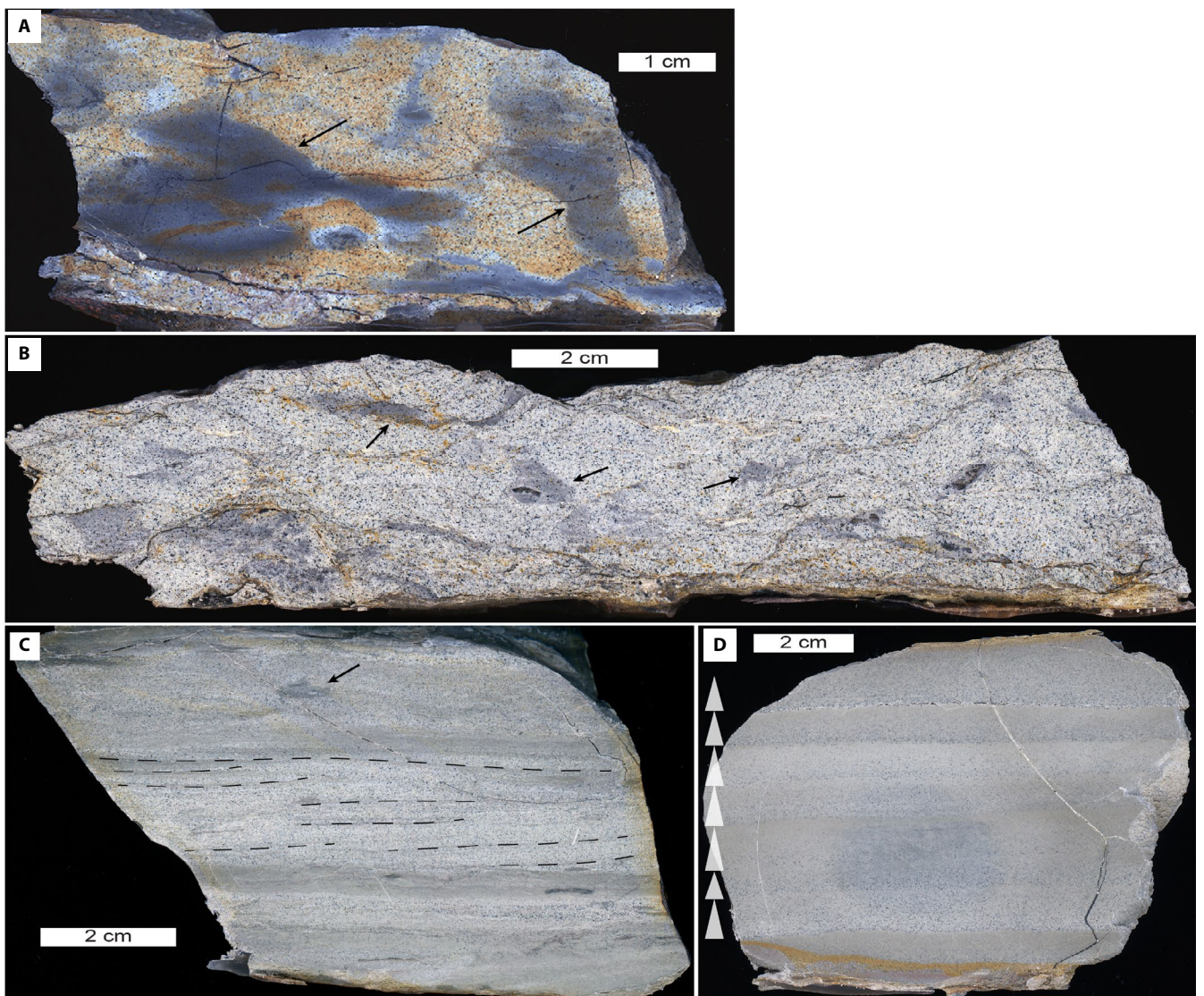


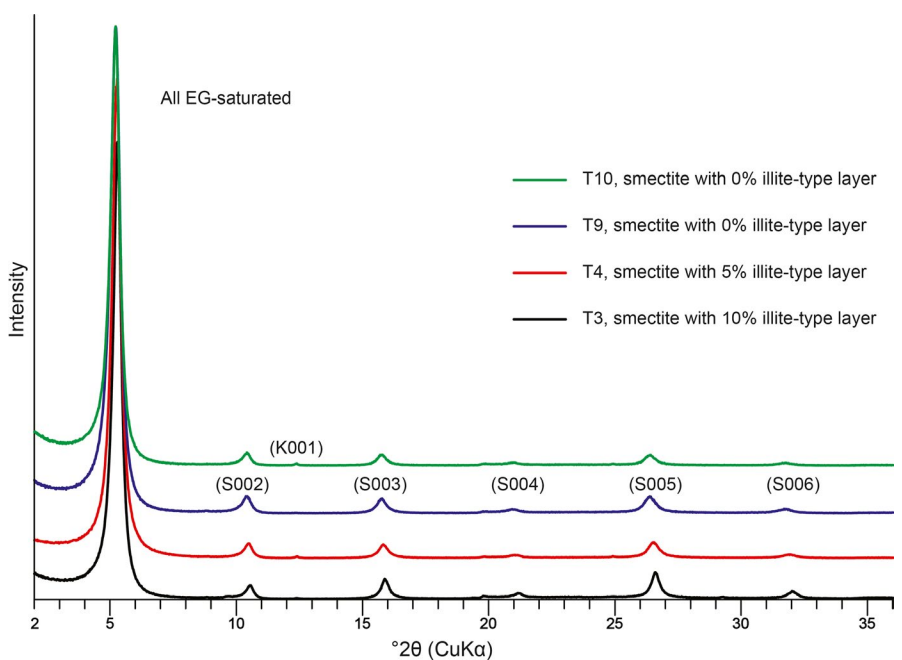
FIGURE 3 Scanned and processed images of polished slabs showing the sedimentary and biogenic features in different bentonite beds in the Tununk Shale. A) Part of bentonite T3 is commonly bioturbated and shows navichnia traces (black arrows). B) Part of bentonite T4 is slightly to commonly bioturbated and shows navichnia traces (black arrows). The abundant black specks revealed on the surface are biotite. C) Part of bentonite T9 shows unidirectionally dipping foresets (dashed lines) under a rather symmetrical crest, indicating influence by storm-induced bottom currents during its deposition. The upper part of this sample is slightly bioturbated (black arrow). D) Part of bentonite T10 shows stacked normal grading (stacked triangles). Although bentonite T9 in C) show sedimentary features indicating reworking by bottom currents, the smectite in this bentonite does not contain any illite-type layers, similar to the smectite in T10 in D)

the fine-grained matrix (Figure 9); and (c) in pore spaces (both intergranular and intragranular) (Figure 10). This paper uses the term 'fine-grained matrix' to refer to the fine-grained groundmass (clay mineral-dominated, with clay to fine-silt-sized particles) in shale samples of the Tununk Shale. Framework grains (medium-silt to sand-sized grains/aggregates) in shale samples usually have different compositions from their surrounding fine-grained matrix.

The clay-dominated composite particles comprise two types, namely altered volcanic rock fragments and shale lithics. Altered volcanic rock fragments were the most commonly observed type in the Tununk Shale (Figure 8A). Volcanic

rock fragments contain dominantly smectite characterized by a highly crenulated morphology, the same as observed in bentonites (Figure 8B). Some volcanic rock fragments contain micron-sized (up to 15 µm) mineral grains such as potassium-feldspar, plagioclase, biotite, quartz, apatite and ilmenite, which are also common phenocrysts in bentonites (Figures 5 and 8B). The other important type of clay-dominated composite particles is shale lithics. Shale lithics contain silt-sized minerals (mostly quartz) scattered in a clay mineral-dominated matrix (Figure 8C,D). The clays in shale lithics are characterized by a more wavy-planar fabric (Figure 8D), compared with the highly crenulated morphology of

FIGURE 4 Representative X-ray diffraction patterns of the $<2\text{ }\mu\text{m}$ fractions in bentonite samples. All are ethylene glycol solvated. See Figure 4 for stratigraphic locations of different bentonite beds. S: smectite, K: kaolinite



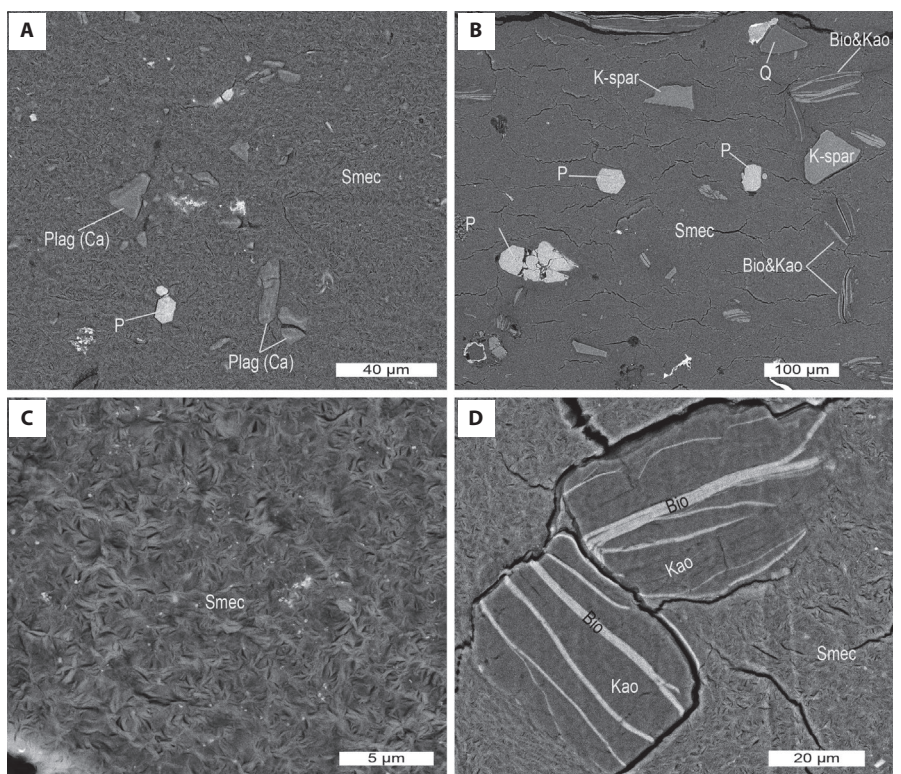
smectite in bentonites and volcanic rock fragments. Because shale lithics show more distinct potassium peaks in SEM-EDS analyses when compared to smectite in bentonites, the clays in shale lithics are identified as mixed-layer I/S. Shale lithics show resistance to compaction and have textural characteristics of fully compacted mudstones, such as preferred orientation of clays and scattered fine silt grains (Figure 8C).

Clays in the fine-grained matrix of the Tununk Shale consist dominantly of mixed-layer I/S, as suggested by XRD data and SEM images (Figures 6B and 9). Under the

SEM, the clay mineral-dominated matrix in shales close to bentonites resembles more the pure smectite of the bentonites (Figure 7), probably a reflection of the comparatively small amounts of illite-type layers in the mixed-layer I/S (Figure 6A). Small amounts of kaolinite are locally present in the clay mineral-dominated matrix of shales (Figure 9D).

The intragranular pore space within foraminifera chambers in the CSSM and SCM lithofacies associations can be filled with smectite and kaolinite (Figure 10A and C), in addition to

FIGURE 5 Characteristic features of un-reworked bentonites (altered volcanic ash) in the Tununk Shale under the SEM. A) and B) Overview of the mineral composition and texture of the bentonite in the Tununk Shale (both are backscatter electron images). Phenocrysts present in the bentonite include common potassium-feldspar (K-spar), biotite (Bio), and small amounts of quartz (Q) and apatite (P). Most kaolinite (Kao) occurs along cleavages of biotite in the bentonite. The clay-dominated matrix is mostly smectite (Smec). C) A closer view showing the highly crenulated morphology of smectite in bentonites. D) A closer view showing kaolinite forming along the cleavages of biotite flakes (relatively lighter-coloured). All are backscatter electron images



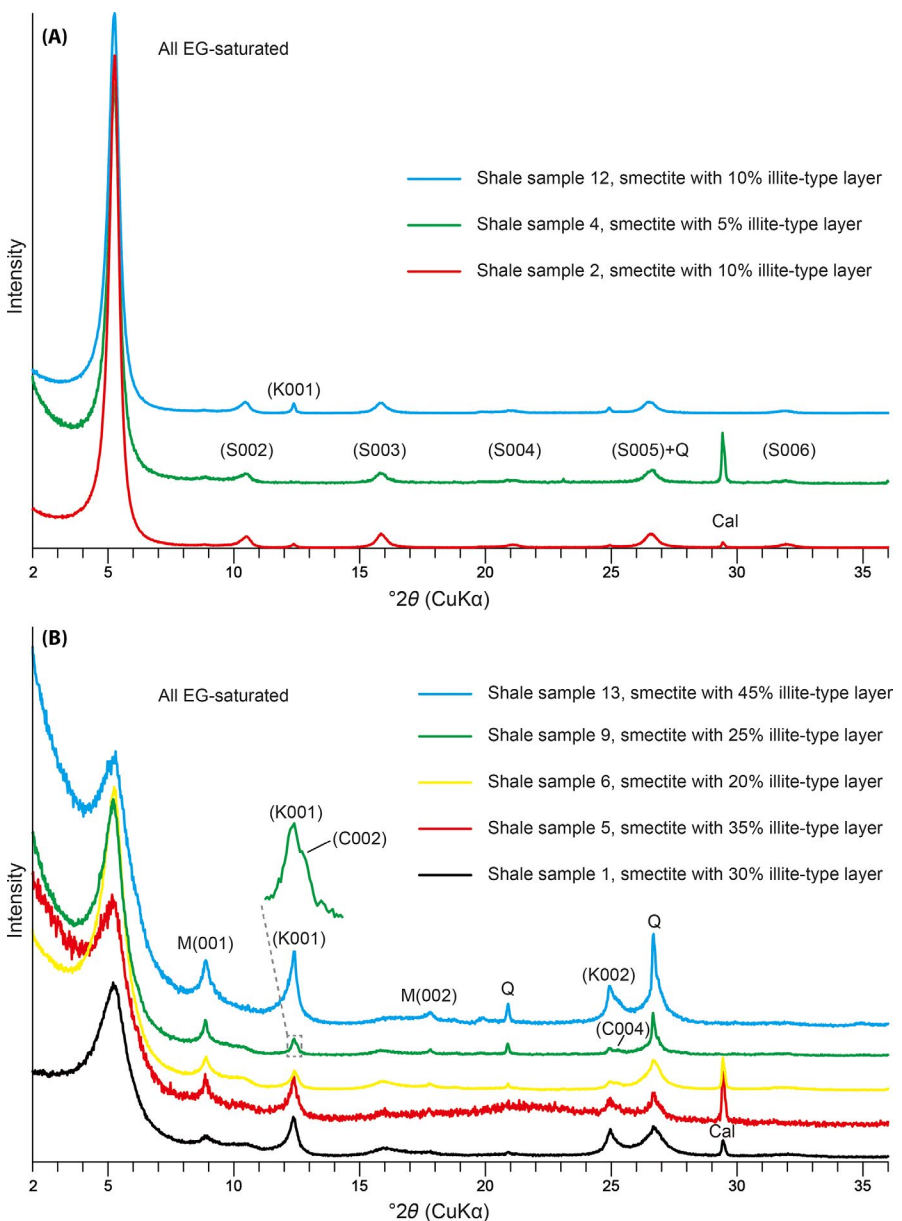


FIGURE 6 A) Representative X-ray diffraction patterns of the $<2 \mu\text{m}$ fractions in shale samples right above (within 20 cm) bentonite beds. All are ethylene glycol solvated. Samples 2, 4 and 12 are from the CSSM, SCM and SSM lithofacies, respectively. The SCM lithofacies has the greatest proportion of sediments derived from carbonate productivity. Therefore, sample 4 shows the strongest relative intensity of the calcite (Cal) peak (due to micron-sized coccoliths). B) Representative X-ray diffraction patterns of the $<2 \mu\text{m}$ fractions in shale samples located far from ($>1 \text{ m}$) bentonite beds. All are ethylene glycol solvated. Samples 1, 5, 6, 9 and 13 are from the CSSM, SCM, CMS, SSM and SSM lithofacies, respectively. The ratio between intensities of the quartz (Q) and calcite (Cal) reflects the relative proportion of sediments derived from terrigenous input (siliciclastic) versus carbonate productivity. See Figure 4 for stratigraphic locations of different bentonite beds. S: smectite, K: kaolinite, M: micaC: chlorite

commonly being filled with early diagenetic calcite (Figure 10A). Kaolinite in the CMS and SSM lithofacies associations more commonly fills the intergranular pore space of silty/sandy laminae (Figure 10E and F). Locally, small amounts of chlorite occur associated with kaolinite, filling particularly large intergranular pore spaces. Kaolinite can also be present along cleavages of biotite flakes in shales (Figures 9B and 10D), similar to what is observed in bentonites (Figure 5B and D).

5 | DISCUSSION

5.1 | Volcanic contributions to the Tununk Shale

Bentonites are the product of early diagenetic alteration to volcanic ash in marine environments (Fisher and Schmincke, 1984; Bohor and Triplehorn, 1993; De Ros

et al., 1997). The original transport of these ashes to the marine environment was probably by wind and episodic (Slaughter and Hamil, 1970; Nadeau and Reynolds, 1981b). Most bentonite beds in the Tununk Shale show reworking by bioturbation or bottom currents (Figure 3). The navicula traces observed in some bentonite samples imply that the incoming volcanic ash was mixed with muds that represent the background sedimentation (muds deposited by suspension settling or bottom currents) (Figure 3A and B). Ripple-scale cross lamination and basal erosional scour associated with some bentonite beds attest to bottom currents and relatively rapid sedimentation (Figure 3C). The stacked normally graded beds in bentonite T10 (Figure 3D) are interpreted to reflect multiple pulses of ash settling during a single volcanic event (Fisher and Schmincke, 1984), in the context of its lateral continuity and similar appearance across the study area.

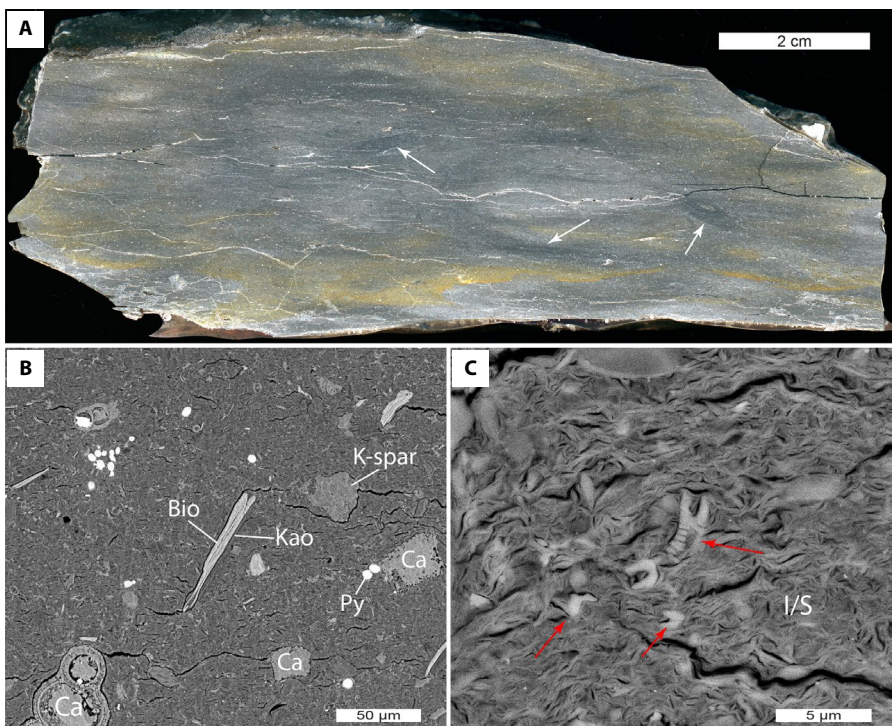


FIGURE 7 Sedimentologic and petrographic facies characteristics of shale samples directly above bentonites. A) Scanned and processed images of the polished slab made of shale sample 2, which lies directly above bentonite T3 (see Figure 4 for stratigraphic locations). This sample is commonly disrupted by navichnia traces (black arrows). The lighter-coloured zones on the polished surface are probably due to mixing of volcanic ashes by benthos. B) An overview of the shale sample shown in A) under the SEM showing the mixture of volcanic ash (smectite-dominated matrix) and background sediments (foraminifera tests and fossil fragments). The potassium-feldspar (K-spar) and biotite (Bio) and related kaolinite (Kao) can be derived from reworking of bentonite T3, lying directly below this sample. C) A closer view of the fine-grained matrix in B). The clays very much resemble the smectite in un-reworked bentonites (high crenulated morphology), which is consistent with the mixed-layer I/S with only 10% illite-type interlayer suggested by the XRD analysis. The mixing of volcanic ash and background sediment (source of mixed-layered I/S) is indicated by the presence of coccolith debris (red arrows). Both B) and C) are backscatter electron images. Ca: calcite, Py: pyrite, I/S: mixed-layer I/S

The preserved stacked normally graded beds in bentonite T10 are suggestive of passive settling and rapid burial (Figure 3D; Bentley and Nittrouer, 2003; Wheatcroft and Drake, 2003), and imply that it has not been reworked by bottom currents or bioturbation. The absence of illite-type layers in the $<2\text{ }\mu\text{m}$ fraction from this bentonite indicates that the smectite has not undergone post-burial transformation to mixed-layer I/S, consistent with the relatively low vitrinite reflectance ($R_o < 0.6\%$; Schamel, 2008) and inferred shallow burial history of the Tununk Shale in the study area (Nadeau and Reynolds, 1981a; Sethi and Leithold, 1994). Because of this, the combined presence of navichnia traces and mixed-layer I/S with only small amounts of illite-type layers in some bentonite beds is interpreted as the result of mixing of volcanic ash with background sediment (e.g. bentonites T3 and T4 in Figures 3A,B and 4). The bioturbated texture of these bentonites indicates relatively slow sedimentation (Savrda and Bottjer, 1991; MacEachern *et al.*, 2005), allowing sufficient time for benthic organisms to mix volcanic ash and background sediments. In contrast, smectite in bottom-current-reworked bentonite T9 (Figure 3C) does not contain any illite-type layers (Figure 4). That this ash layer was not

noticeably ‘contaminated’ by background sediment implies that ash deposition and burial occurred rapidly (Bentley and Nittrouer, 2003; Wheatcroft and Drake, 2003), forestalling significant biological reworking. Whereas the bentonite beds preserved in the Tununk Shale are visual markers of episodic volcanic input, an apparent visual absence of bentonite beds should not be construed as an absence of volcanic input. When bottom currents are energetic enough to completely rework and disperse incoming ash materials, or when intense bioturbation fully mixes them with background sediment, no distinct bentonite layer will remain in the rock record. Instead, all the volcanic input would be so intimately mixed with the background sediments that its recognition requires petrographic identification of altered volcanic rock fragments in shale samples (Figures 8A,B and 11).

Bentonite beds in shale successions can be viewed as ‘internal standards’ for evaluating the degree of burial metamorphism in shales because their source is distinct from the shale they are found in. The smectite in un-reworked bentonites in the Tununk is characterized by a lack of illitization, indicating that the associated shales should as well have undergone negligible illitization after deposition (Schultz, 1978).

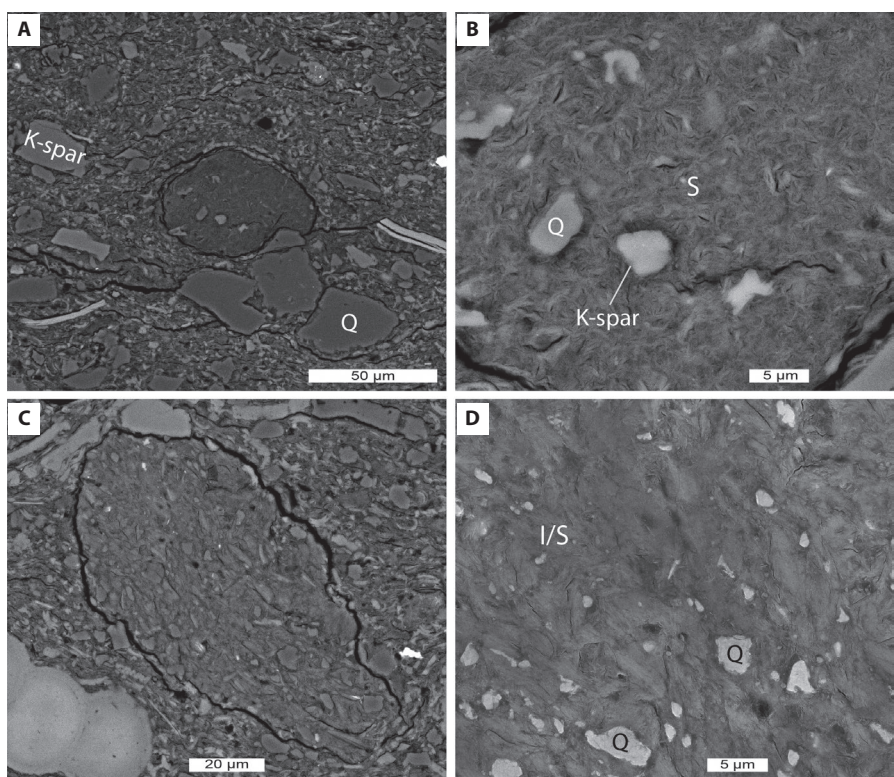


FIGURE 8 Characteristics of the two types of clay-dominated composite particles (aggregates) that are commonly present in all lithofacies types throughout the Tununk Shale. A) One altered volcanic rock fragment present in an area of the CSSM lithofacies. The lower right corner of the volcanic rock fragment is slightly indented by a harder quartz grain (Q), and there is differential compaction around the volcanic rock fragment. B) Closer view of the volcanic rock fragment in A). This volcanic rock fragment contains micron-sized quartz and potassium-feldspar (K-spar) in a matrix dominated by smectite (note the crenulated morphology), and has essentially the same composition and texture as bentonites (see Figure 7). C) One shale lithic present in an area of the CSSM lithofacies. Note the distinct difference in composition between the shale lithic (non-calcareous) and its enclosing calcareous fine-grained matrix (cocolith debris indicated by red arrows). D) Closer view of the shale lithic in C). This shale lithic contains common fine silt grains (mostly quartz) and clays. The EDS spectrum for the clays in this view shows Si, Al, K, Mg and Fe, in decreasing levels. Integrated with a more filamentous morphology, the clays are recognized as mixed-layer I/S. The preferred orientation of this shale lithic indicates that it was consolidated before deposition. A)–C): backscatter electron mode; D): secondary electron mode

Therefore, the randomly interstratified I/S in shale samples must be detrital and existed prior to deposition in the Tununk system. Similarly, the relatively low amount of illite-type layers in the mixed-layer I/S from shales adjacent to bentonites is probably indicative of a volcanic ash – background sediment mixing effect that diminishes away from the ash bed. This interpretation is consistent with the bioturbated nature and the highly similar smectite-dominated texture of these shale samples (Figure 7).

5.2 | Origins of other clay minerals in the Tununk Shale

Shales located at some distance (>1 m) above bentonite beds contain dominantly mixed-layer I/S with a distinctly higher proportion of illite-type layers than shale samples close to bentonites. This probably reflects the volumetric dominance of detrital-terrigenous matrix I/S over smectite-dominated altered volcanic rock fragments (Figure 9).

The mixed-layer I/S in shales has multiple possible sources (Figure 11). It can for example be derived from various older shale/mudstone successions in the hinterland, an interpretation that is consistent with the presence of shale lithics in the Tununk Shale. Other possible sources for the mixed-layer I/S are soil profiles developed on older volcanic rocks and weathering of volcanic debris that fell on land areas and underwent repeated wetting and drying episodes (Hein and Scholl, 1978; Schultz, 1978; Eberl *et al.*, 1987; Kemp *et al.*, 2016).

In XRD patterns from the Tununk shale samples, the symmetrical peak at $\sim 10 \text{ \AA}$ indicates the presence of mica instead of discrete illite in the $<2 \mu\text{m}$ fractions (Środoń, 1981). The SEM analysis shows that biotite is the dominant type of mica in the Tununk Shale. Because biotite is a common phenocryst in bentonites (Figures 3B and 5B), the biotite in shales may be derived from resuspension and redeposition of volcanic ash in the marine environment as well as from terrigenous sources (also probably supplying some muscovite).

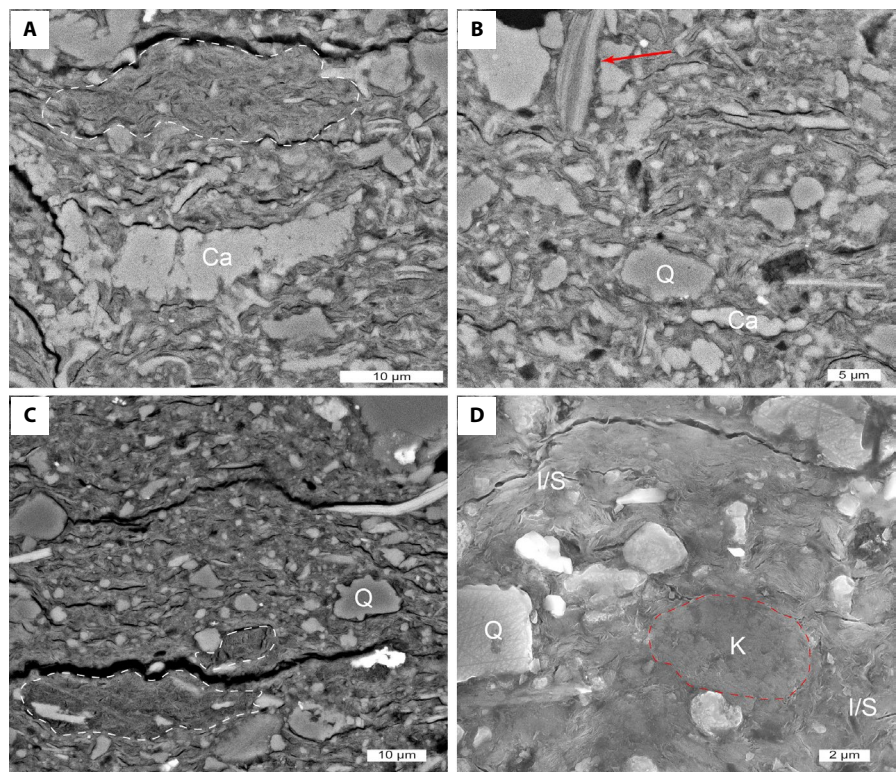


FIGURE 9 Clay minerals present in the fine-grained matrix in the Tununk Shale. A) An area in the SCM lithofacies showing a small altered volcanic rock fragment (white-dashed outlines, smectite-dominated) and shell fragments (Ca) in the fine-grained matrix consisting of coccolith debris and mixed-layer I/S. B) An area in the CMS lithofacies showing common siliciclastic grains including quartz and biotite (and related kaolinite, red arrow) in the fine-grained matrix consisting dominantly mixed-layer I/S and a small amount of coccolith debris. C) An area showing common quartz silt and two smectite-dominated volcanic rock fragments (white-dashed outlines) in the non-calcareous matrix in the SSM lithofacies. D) Closer view of the clay mineral-dominated matrix in the SSM lithofacies. The matrix consists dominantly of mixed-layered I/S and a small amount of kaolinite. The mixed-layer I/S consists of flaky, ragged crystals with some filamentous margins. The kaolinite (within red-dashed lines) is possibly of detrital origin

Most (>90%) kaolinite recognized under the SEM in the Tununk shale samples occurs as pore-filling cements and therefore formed during early diagenesis before significant compaction (Figures 10 and 11). Possible sources of silica for kaolinite authigenesis in the Tununk Shale are the silicon present as dissolved (probably present as $\text{Si}(\text{OH})_4$) and particulate (a wide variety of silicate and aluminosilicate minerals) forms in sea water (Chester, 2009), as well as alteration in volcanic ash particles. The transformation from volcanic glass to smectite is generally thought to occur during early diagenesis and can release silicon (Fisher and Schmincke, 1984). Due to the extremely low solubility of aluminium in sea water, aluminium is primarily present in particulate form in aluminosilicate minerals and hydrous aluminium oxides (Michalopoulos and Aller, 1995). The breakdown of organic carbon by bacterial sulphate reduction (indicated by the presence of pyrite) and methanogenesis is typically associated with high concentrations of organic acids in the sediment interstitial waters (Barcelona, 1980; Gunnarsson and Rönnow, 1982; Surdam *et al.*, 1989; Manning *et al.*, 1994; Macquaker *et al.*, 2014). These acids can promote the dissolution of unstable aluminosilicates

(e.g. biotite, feldspars, unstable clays and volcanic detritus), volcanic glass and hydrous aluminium oxides and thus result in localized availability of aluminium (Moncure *et al.*, 1984; Surdam and Crossey, 1985; Acker and Bricker, 1992; Fein, 1994). Kaolinite can then precipitate from interstitial solutions in intergranular and intragranular pore spaces (Figure 10B,C,E), along the cleavages of biotite flakes (Figure 10D), and as replacement of unstable detrital grains (Figure 10F). In the Tununk Shale, the precipitation of kaolinite was not accompanied by significant carbonate dissolution (e.g. dissolution of foraminifera tests), suggesting that kaolinite authigenesis, rather than carbonate dissolution, was the main acid buffer mechanism in its sediment interstitial waters (Macquaker *et al.*, 2014).

Only a small amount of chlorite is present as pore-filling cements in relatively few shale samples. The precipitation of chlorite in the Tununk Shale probably was limited by the availability of iron and magnesium in interstitial waters. Because pyrite forms very early in diagenesis, the common presence of pyrite in the Tununk Shale (Figure 10B and D) indicates that reduced iron in interstitial waters was largely removed before favourable conditions for chlorite precipitation

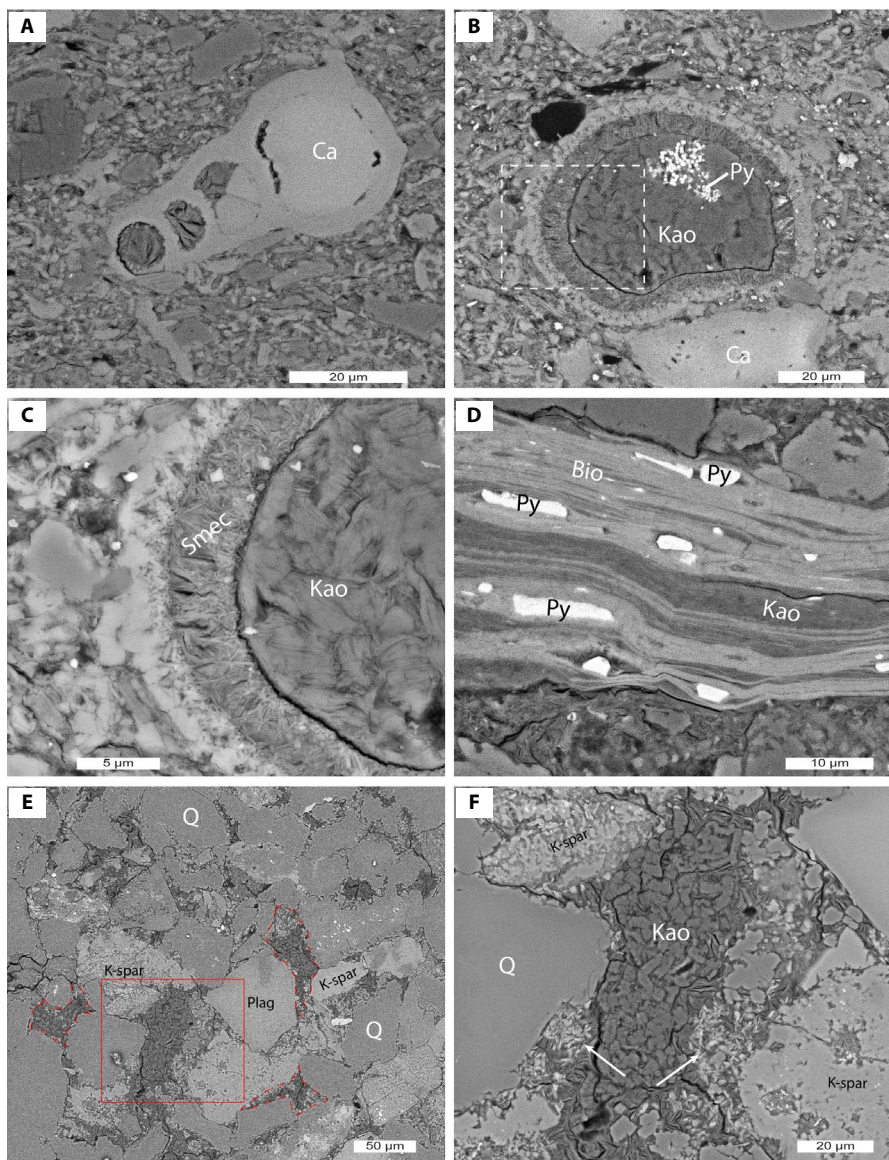


FIGURE 10 A) A foraminifera test in the SCM lithofacies is filled with authigenic smectite and calcite. B) A foraminifera test in the SCM lithofacies is filled with authigenic smectite, kaolinite and pyrite. C) Closer view of the dashed area in C). Authigenic smectite formed prior to authigenic kaolinite. D) Closer view in the CSM lithofacies showing authigenic kaolinite and pyrite forming along the cleavages within biotite. E) Presence of common authigenic kaolinite (within red-dashed lines) and a minor amount of chlorite in the pore space within a silty/sandy lamina in the SSM lithofacies. F) Closer view of the area within the red square in E). Note booklet-like kaolinite and plate-like chlorite (white arrows). This pore is larger than others surrounding it, and both the pore and its kaolinite and chlorite fill may be the result of dissolution of a feldspar grain or a volcanic detritus. Ca: calcite; Smec: smectite; Kao: kaolinite; Bio: biotite; Py: pyrite; K-spar: potassium-feldspar; Plag: plagioclase; Q: quartz

were reached. Furthermore, the authigenesis of smectite from alteration in volcanic glass or unstable volcanic debris, which occurred prior to kaolinite formation (Figure 10A through C), requires significant incorporation of magnesium (Fisher and Schmincke, 1984). It is therefore probable that chlorite was only precipitated at places where silicon, aluminium, iron and magnesium derived from dissolution of unstable volcanic materials (e.g. mafic minerals) were sufficiently retained at a local scale (Figure 10F; Anjos *et al.*, 2003).

5.3 | Implications for using clay mineral assemblages as proxies for palaeoclimate and burial history

Clay mineralogy has been widely used as a proxy for quantifying the intensity of continental weathering and reconstructing palaeoclimate (Singer, 1984; Dera *et al.*, 2009; Kemp *et al.*, 2016; Wendler *et al.*, 2016). The most important underlying

assumption for this approach is that the clay minerals in a given sedimentary succession are derived mainly from coeval soils and thus directly reflect climate parameters (weathering conditions) in the hinterland (Biscaye, 1965; Singer, 1984; Chamley, 1989; Thiry, 2000; Junntila *et al.*, 2005; Wendler *et al.*, 2016). A previous study of clay minerals in the Tropic Shale and Tununk Shale in southern Utah (south of the study area) reported that detrital clays include kaolinite, discrete illite (mica), chlorite and mixed-layer I/S (Sethi and Leithold, 1994). Results from this study, however, based on comparisons between clay mineral assemblages of bentonites and shales, suggest that the dominant land-derived detrital clay mineral in the Tununk Shale is mixer-layer I/S, whereas kaolinite and chlorite are mostly authigenic and mica (dominantly biotite) is mainly associated with volcanic ash falls. More importantly, only the mixed-layer I/S derived from weathering of volcanic rocks and volcanic ash deposited on land may have a bearing on weathering conditions in the hinterland.

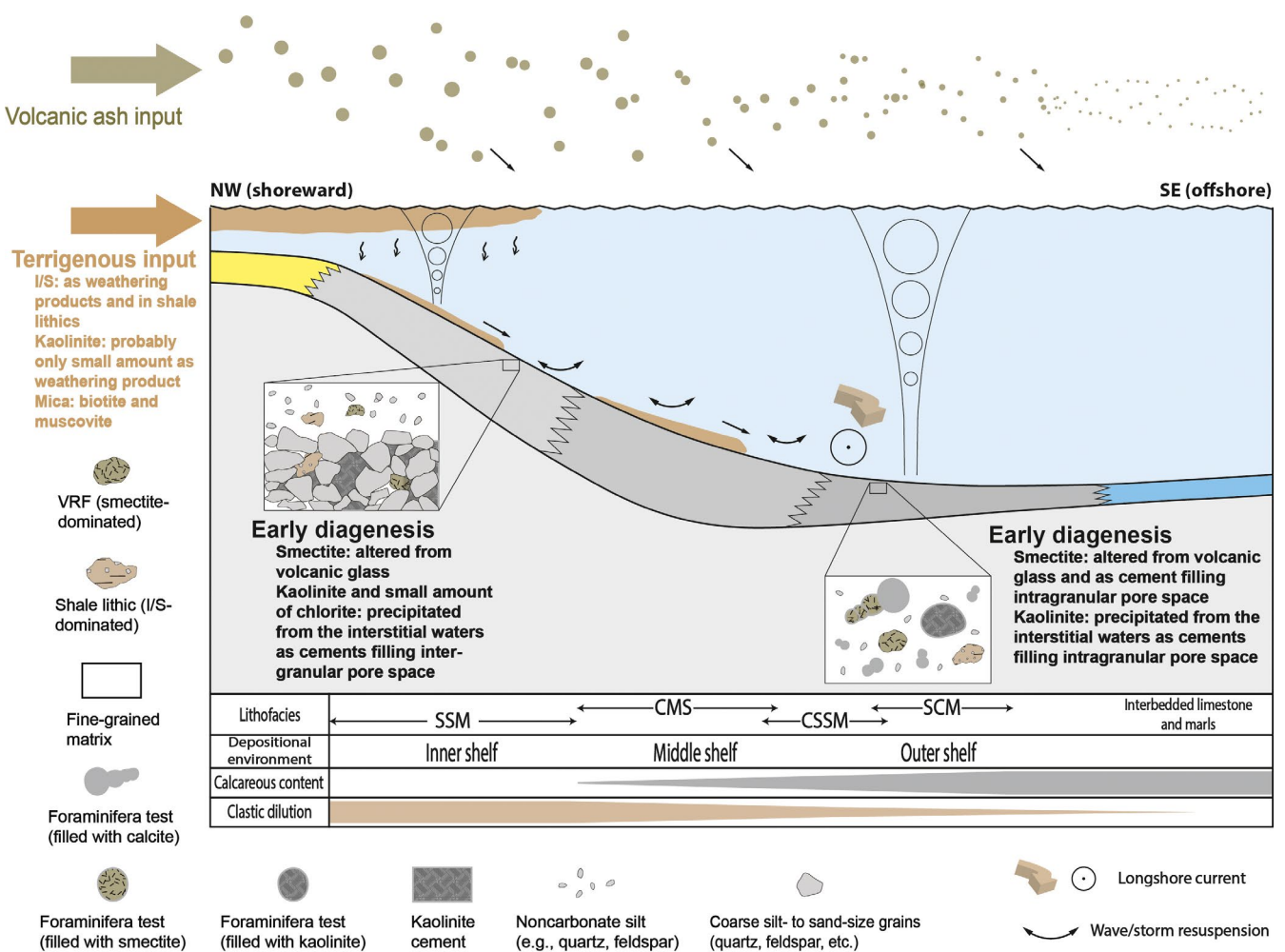


FIGURE 11 Schematic drawing of the dispersal processes and origins of clay minerals in the Tununk system. The smectite in shales is largely derived from alteration in volcanic ash in the marine environment during early diagenesis. The mixed-layer I/S in shales can be derived from weathering of volcanic debris that had been deposited in the hinterland and from older mudstones/shales (as suggested by the presence of shale lithics). Shale lithics in the Tununk Shale have two possible sources, including disintegration of exposed older mudstone successions in the hinterland and the unconformity located updrift of the study area (then dispersed by southward-directed longshore currents). A significant amount of kaolinite (and trace amount of chlorite) was precipitated as early diagenetic cements in the pore spaces, instead of being introduced as weathered terrestrial detritus via river run-off

In contrast, the mixed-layer I/S derived from recycled mudstones that experienced burial metamorphism, signified by shale lithics seen in SEM petrography, has no relation to the weathering regime at the time of deposition. In the context of palaeogeographic reconstructions (Figure 1), shale lithics in the Tununk Shale have two possible sources. The first source is the rapid erosion of areas with high relief (disintegration of exposed older mudstone successions by mechanical weathering). The second potential source is the lacuna located updrift of the study area (Figure 1A). The lacuna was associated with a submarine unconformity from which the previously deposited Cenomanian marine shales (probably also containing volcanic input) were removed through erosion and reworked by wave-induced currents (Ryer and Lovekin, 1986). Although there is some uncertainty regarding the source of shale lithics, clay minerals in these recycled

mudstone fragments cannot possibly be related to palaeoclimate conditions that prevailed during the deposition of the Tununk Shale.

As discussed above, micas (dominantly biotite) in the Tununk Shale can be derived from either wind-borne volcanic ash or terrigenous input. Significant amounts of kaolinite and chlorite were directly precipitated from pore waters as early diagenetic cements, instead of being introduced as weathered terrestrial detritus via river run-off. It is therefore difficult, if not impossible, to determine the detrital contribution of mixed-layer I/S, mica, kaolinite, and chlorite to the Tununk Shale and then to use relative proportions of these clays to infer palaeoclimate in the hinterland. The mixing of sediments derived from different sources, as well as early diagenetic contributions and overprint, significantly obscures the original detrital clay mineral assemblages of marine

mudstone successions. When attempting to interpret the palaeoclimate based on clay mineral assemblages in marine mudstone successions, one needs to focus only on clay minerals derived from coeval soils, factoring out clays derived from volcanic input, recycled sediments and early diagenesis.

In the pelagic deposits of the Bridge Creek Limestone Member of central Colorado, time-equivalent to the Tununk Shale and deposited in the central part of the WIS, discrete illite and mixed-layer I/S were considered as detrital and volcanic in origin, respectively, because bentonites in the Bridge Creek Limestone also contain mixed-layer I/S (Pratt, 1984). The mismatch between the detrital clay mineral assemblages in the distal Bridge Creek Limestone (discrete illite suggested by Pratt, 1984; Eicher and Diner, 1989) and the proximal Tununk Shale (abundant detrital-terrigenous matrix I/S) indicates that clay mineral assemblages in the Bridge Creek Limestone were probably modified after deposition. For example, the mixed-layer I/S in the commonly bioturbated bentonites from the Bridge Creek Limestone (Elder, 1985) could be due to mixture of volcanic ash with background sediments, similar to what was observed in the Tununk Shale. However, alteration during burial metamorphism may be a more plausible explanation for the observed mixed-layer I/S because analysis of the clay mineralogy in the Smoky Hill Shale Member of the Niobrabra Formation (stratigraphically higher than the Bridge Creek Limestone) in the same area (Pueblo, Colorado) indicate burial temperatures between 70 and 100°C (Pollastro and Martinze, 1985). Being stratigraphically lower, the Bridge Creek Limestone should have experienced even higher burial temperatures, making it probable that the observed mixed-layer I/S compositions are not a detrital signature and thus of dubious value as a palaeoclimate proxy.

The progressive conversion of smectite into illite with increasing depth has been widely recognized (Burst, 1957; Perry and Hower, 1970; Schultz, 1978), and allows the degree of illitization in shales to be used as a geothermometer (Huang *et al.*, 1993; Pollastro, 1993; Price and McDowell, 1993; Hillier *et al.*, 1995; Uysal *et al.*, 2000). Results from this study demonstrate that the mixing of sediments from multiple sources severely complicates deciphering the illitization history of sedimentary successions and its application to infer burial and thermal histories. Shales containing a high proportion of material derived from recycled sediments could have a ‘head start’ in the illitization process (Rettke, 1981), compared with those that are dominated by higher proportions of volcanic ash input, because the kinetics of the smectite-to-illite reaction appears to be more sensitive to the time available for the process than to the actual burial temperature (Eberl *et al.*, 1987; Hillier *et al.*, 1995). Many studies of ancient mudstone successions containing bentonites show that the mixed-layer I/S in shales usually contains a greater amount of illite-type layers compared with mixed-layer I/S or smectite in associated bentonites (Schulz, 1978; Sucha *et al.*,

1993; Hillier *et al.*, 1995). On one hand, some researchers have attributed this difference to delayed illitization of smectite in the bentonite (Li *et al.*, 1997). On the other hand, in the Pierre Shale of the northern Great Plains region, comparison of the clay minerals in the bentonite and host shales that had different burial histories shows no appreciable tendency for bentonite to lag behind shales during illitization (Schulz, 1978). The difference in the amount of illite-type layers in the mixed-layer I/S between bentonites and associated shales is therefore more probably the result of higher proportions of recycled sediments in shales (Sucha *et al.*, 1993). Therefore, if one wants to use mixed-layer I/S compositions in a given sedimentary succession to infer thermal regimes, the complex sources of clay minerals have to be taken into consideration. Careful petrographic examination and selection of samples without shale lithics should help elucidate the clay mineral signals that reflect burial history from those influenced by recycled sediments.

6 | CONCLUSIONS

The origin of clay minerals in the Upper Cretaceous Tununk Shale Member of the Mancos Shale in south-central Utah is complex. Through integration of sedimentologic, petrographic and clay mineralogical analysis, however, this complexity can be evaluated and clay mineral origins can be decoded. The main conclusions from this study are:

1. In the Tununk Shale, the phyllosilicate content of bentonites consists of abundant smectite (>80%) and minor amounts of biotite and kaolinite. The smectite in the bentonites reflects alteration in volcanic glass in the marine environment. Bentonites can be reworked and mixed with background sediment by benthic bioturbation and bottom currents. The pure nature of smectite (containing no illite-type layers) in un-reworked bentonites indicates a lack of illitization during burial, and by extension, that burial illitization of smectite in associated shales should be negligible.
2. Clays in Tununk Shale beds consist dominantly of mixed-layer illite/smectite (I/S) with up to 45% illite-type layers, small amounts of kaolinite and mica, and sometimes trace amounts of chlorite. The SEM examination indicates that the clay minerals in shales occur in three forms: (a) within clay-dominated composite particles (or aggregates); (b) in the fine-grained matrix; and (c) within pore spaces (both intergranular and intragranular).
3. The most abundant types of clay-rich composite particles in the Tununk Shale are altered volcanic rock fragments (dominated by smectite) and shale lithics (dominated by mixed-layer I/S). Altered volcanic rock fragments in shales were most probably derived from re-suspended

and re-deposited volcanic ash particles (volcanic glass), judging from their compositional and textural similarity to bentonites. Shale lithics can plausibly be derived from (a) erosion of older mudstone successions exposed in the hinterland and (b) submarine erosion at the unconformity located updrift of the study area.

4. Integrating XRD data with petrographic observations suggests that mixed-layer I/S, the dominant clay mineral in these shales, can be plausibly derived from older mudstones/shales (as suggested by the presence of shale lithics) and from soil profiles developed on older volcanic rocks and weathering of volcanic debris that had been deposited in the hinterland. The biotite in shales can be attributed to reworking and redistribution of volcanic ashes in the marine environment as well as to terrigenous input (also supplying some muscovite). A significant amount of kaolinite and chlorite was precipitated as early diagenetic cements in the pore spaces.
5. Clay minerals in the Tununk Shale were derived from multiple sources. These include terrigenous input (weathering products and recycled sediments), wind-borne volcanic ash, intrabasinal erosion, and early diagenesis. The example of the Tununk Shale serves to illustrate that complex origins of clay minerals in marine mudstone successions place significant limitations on the use of clay mineral assemblages to infer palaeoclimate and for the reconstruction of burial and thermal histories (based on the progressive conversion from smectite to illite). For best results, clay mineralogical analysis must be integrated with careful studies of sedimentologic and petrographic characteristics, so that a comprehensive understanding of the origin of clay minerals in fine-grained sedimentary successions may be obtained.

ACKNOWLEDGEMENTS

We thank João P. Trabucho, Kevin Taylor and Editor Peter Swart for their valuable comments and suggestions on the manuscript. Comments by Dr. Joe Macquaker and Dr. Kevin Bohacs on an earlier version of the manuscript are also appreciated. This research was supported by the sponsors of the Indiana University Shale Research Consortium (Anadarko, Chevron, ConocoPhillips, ExxonMobil, Shell, Statoil, Marathon, Whiting and Wintershall). Additional support was provided through student research grants and fellowships awarded to Zhiyang Li by the Geological Society of America, SEPM (Society for Sedimentary Geology), American Association of Petroleum Geologists (Donald A. and Mary O'Nesky Named Grant), and the Indiana University Department of Geological Sciences (Grassman Fellowship). Many thanks to Sue Fivecoat and John Reay from the Bureau of Land Management (BLM) at Henry Mountains Field Station for their guidance and help on granting us permission

for fieldwork in the study area. We also thank Bei Liu, Britt Rossman and Matthew Leung for their assistance in the field.

CONFLICT OF INTEREST

The authors have no conflict of interest to declare.

DATA AVAILABILITY STATEMENT

The data that support the findings of this study are available from the corresponding author upon reasonable request.

REFERENCES

- Acker, J.G. and Bricker, O.P. (1992) The influence of pH on biotite dissolution and alteration kinetics at low temperature. *Geochimica et Cosmochimica Acta*, 56(8), 3073–3092. Available at: doi:[https://doi.org/10.1016/0016-7037\(92\)90290-Y](https://doi.org/10.1016/0016-7037(92)90290-Y).
- Anjos, S.M.C., de Ros, L.F. and Silva, C.M.A. (2003) Chlorite authigenesis and porosity preservation in the Upper Cretaceous marine sandstones of the Santos Basin, offshore eastern Brazil. In: Worden, R.H. and Morad, S. (Eds.) *Clay Mineral Cements in Sandstones*. Malden, MA: International Association of Sedimentologists Special Publication, Vol. 34, pp. 291–316.
- Aplin, A.C. and Macquaker, J.H.S. (2012) Mudstone diversity: origin and implications for source, seal, and reservoir properties in petroleum systems. *AAPG Bulletin*, 95(12), 2031–2059. Available at: doi:<https://doi.org/10.1306/03281110162>.
- Barcelona, M.J. (1980) Dissolved organic carbon and volatile fatty acids in marine sediment pore waters. *Geochimica et Cosmochimica Acta*, 44(12), 1977–1984. Available at: doi:[https://doi.org/10.1016/0016-7037\(80\)90197-0](https://doi.org/10.1016/0016-7037(80)90197-0).
- Barron, E.J. (1989) Severe storms during earth history. *Geological Society of America Bulletin*, 101(5), 601–612. Available at: doi:[https://doi.org/10.1130/0016-7606\(1989\)101<0601:SSDEH>2.3.CO;2](https://doi.org/10.1130/0016-7606(1989)101<0601:SSDEH>2.3.CO;2).
- Barron, E.J., Arthur, M.A. and Kauffman, E.G. (1985) Cretaceous rhythmic bedding sequences: a plausible link between orbital variations and climate. *Earth and Planetary Science Letters*, 72(4), 327–340. Available at: doi:[https://doi.org/10.1016/0012-821X\(85\)90056-1](https://doi.org/10.1016/0012-821X(85)90056-1).
- Bentley, S.J. and Nittrouer, C.A. (2003) Emplacement, modification, and preservation of event strata on a flood-dominated continental shelf: Eel shelf, Northern California. *Continental Shelf Research*, 23(16), 1465–1493. Available at: doi:<https://doi.org/10.1016/j.csr.2003.08.005>.
- Berner, R.A. (1984) Sedimentary pyrite formation: an update. *Geochimica et Cosmochimica Acta*, 48(4), 605–615. Available at: doi:[https://doi.org/10.1016/0016-7037\(84\)90089-9](https://doi.org/10.1016/0016-7037(84)90089-9).
- Biscaye, P.E. (1965) Mineralogy and sedimentation of recent deep-sea clay in the Atlantic Ocean and adjacent seas and oceans. *GSA Bulletin*, 76(7), 803–832. Available at: doi:[https://doi.org/10.1130/0016-7606\(1965\)76\[803:masord\]2.0.co;2](https://doi.org/10.1130/0016-7606(1965)76[803:masord]2.0.co;2).
- Bohor, B.F. and Triplehorn, D.M. (1993) *Tonsteins: Altered Volcanic Ash Layers in Coal-Bearing Sequences*. Boulder, Colorado: Geological Society of America. Special Paper 285.
- Burst, J.F.J. (1957) Postdiagenetic clay mineral-environment relationship in the Gulf Coast Eocene. *Clays and Clay Minerals*, 6(1), 327–341.

- Canfield, D.E., Thamdrup, B. and Hansen, J.W. (1993) The anaerobic degradation of organic matter in Danish coastal sediments: iron reduction, manganese reduction, and sulfate reduction. *Geochimica et Cosmochimica Acta*, 57(16), 3867–3883. Available at: doi:[https://doi.org/10.1016/0016-7037\(93\)90340-3](https://doi.org/10.1016/0016-7037(93)90340-3).
- Chamley, H. (1989) *Clay Sedimentology*. Berlin Heidelberg, Germany: Springer-Verlag.
- Chester, R. (2009). *Marine Geochemistry*. Hoboken, NJ: Wiley-Blackwell.
- Clayton, T., Pearce, R.B. and Peterson, L.C. (1999) Indirect climatic control of the clay mineral composition of Quaternary sediments from the Cariaco basin, northern Venezuela (ODP Site 1002). *Marine Geology*, 161(2), 191–206. Available at: doi:[https://doi.org/10.1016/S0025-3227\(99\)00036-5](https://doi.org/10.1016/S0025-3227(99)00036-5).
- Colin, C., Siani, G., Liu, Z., Blamart, D., Skonieczny, C., Zhao, Y. et al. (2014) Late Miocene to early Pliocene climate variability off NW Africa (ODP Site 659). *Palaeogeography, Palaeoclimatology, Palaeoecology*, 401, 81–95. Available at: doi:<https://doi.org/10.1016/j.palaeo.2014.02.015>.
- Curtis, C.D. (1990) Aspects of climatic influence on the clay mineralogy and geochemistry of soils, palaeosols and clastic sedimentary rocks. *Journal of the Geological Society*, 147(2), 351. Available at: doi:<https://doi.org/10.1144/gsjgs.147.2.0351>.
- De Ros, L.F., Morad, S. and Al-Aasm, I.S. (1997) Diagenesis of siliciclastic and volcanioclastic sediments in the Cretaceous and Miocene sequences of the NW African margin (DSDP Leg 47A, Site 397). *Sedimentary Geology*, 112(1), 137–156. Available at: doi:[https://doi.org/10.1016/S0037-0738\(97\)00030-4](https://doi.org/10.1016/S0037-0738(97)00030-4).
- DeCelles, P.G. (2004) Late Jurassic to Eocene evolution of the Cordilleran thrust belt and foreland basin system, western U.S.A. *American Journal of Science*, 304(2), 105–168. Available at: doi:<https://doi.org/10.2475/ajs.304.2.105>.
- DeCelles, P.G. and Coogan, J.C. (2006) Regional structure and kinematic history of the Sevier fold-and-thrust belt, central Utah. *Geological Society of America Bulletin*, 118(7–8), 841–864. Available at: doi:<https://doi.org/10.1130/B25759.1>.
- Dera, G., Pellenard, P., Neige, P., Deconinck, J.-F., Puccéat, E. and Dommergues, J.-L. (2009) Distribution of clay minerals in Early Jurassic Peritethyan seas: palaeoclimatic significance inferred from multiproxy comparisons. *Palaeogeography, Palaeoclimatology, Palaeoecology*, 271(1), 39–51. Available at: doi:<https://doi.org/10.1016/j.palaeo.2008.09.010>.
- DeReuil, A.A. and Birgenheier, L.P. (2019) Sediment dispersal and organic carbon preservation in a dynamic mudstone-dominated system, Juana Lopez Member. *Mancos Shale. Sedimentology*, 66(3), 1002–1041. Available at: doi:<https://doi.org/10.1111/sed.12532>.
- Eberl, D.D., Šrodoň, J. and Northrop, H.R. (1987) Potassium fixation in smectite by wetting and drying. In: Davies, J.A. and Hayes, K.F. (Eds.) *Geochemical Processes at Mineral Surfaces*. Washington, DC: American Chemical Society, Vol. 323, pp. 296–326.
- Eicher, D.L. and Diner, R. (1989) Origin of the cretaceous bridge creek cycles in the western interior, United States. *Palaeogeography, Palaeoclimatology, Palaeoecology*, 74(1), 127–146. Available at: doi:[https://doi.org/10.1016/0031-0182\(89\)90023-0](https://doi.org/10.1016/0031-0182(89)90023-0).
- Elder, W.P. (1985) Biotic patterns across the Cenomanian-Turonian extinction boundary near Pueblo, Colorado. In: Pratt, L.M., Kauffman, E.G. and Zelt, F.B. (Eds.) *Fine-Grained Deposits and Biofacies of the Cretaceous Western Interior Seaway: Evidence of Cyclic Sedimentary Processes*. Tulsa, OK: Society of Economic Paleontologists and Mineralogists, Vol. 4, pp. 157–169.
- Eldrett, J.S., Ma, C., Bergman, S.C., Ozkan, A., Minisini, D., Lutz, B. et al. (2015) Origin of limestone–marlstone cycles: astronomic forcing of organic-rich sedimentary rocks from the Cenomanian to early Coniacian of the Cretaceous Western Interior Seaway, USA. *Earth and Planetary Science Letters*, 423(Supplement C), 98–113. Available at: doi:<https://doi.org/10.1016/j.epsl.2015.04.026>.
- Erickson, M.C. and Slingerland, R.L. (1990) Numerical simulations of tidal and wind-driven circulation in the Cretaceous interior seaway of North America. *Geological Society of America Bulletin*, 102(11), 1499–1516. Available at: doi:[https://doi.org/10.1130/0016-7606\(1990\)102<1499:nstaw>2.3.co;2](https://doi.org/10.1130/0016-7606(1990)102<1499:nstaw>2.3.co;2).
- Fein, J.B. (1994) Porosity enhancement during clastic diagenesis as a result of aqueous metal-carboxylate complexation: experimental studies. *Chemical Geology*, 115(3), 263–279. Available at: doi:[https://doi.org/10.1016/0009-2541\(94\)90191-0](https://doi.org/10.1016/0009-2541(94)90191-0).
- Fisher, R.V. and Schmincke, H.-U. (1984). Berlin, Heidelberg: *Pyroclastic Rocks*. Springer-Verlag.
- Floegel, S., Hay, W.W., DeConto, R.M. and Balukhovsky, A.N. (2005) Formation of sedimentary bedding couplets in the Western Interior Seaway of North America—implications from climate system modeling. *Palaeogeography, Palaeoclimatology, Palaeoecology*, 218(1–2), 125–143. Available at: doi:<https://doi.org/10.1016/j.palaeo.2004.12.011>.
- Froelich, P.N., Klinkhammer, G.P., Bender, M.L., Luedtke, N.A., Heath, G.R., Cullen, D. et al. (1979) Early oxidation of organic matter in pelagic sediments of the eastern equatorial Atlantic: suboxic diagenesis. *Geochimica et Cosmochimica Acta*, 43(7), 1075–1090. Available at: doi:[https://doi.org/10.1016/0016-7037\(79\)90095-4](https://doi.org/10.1016/0016-7037(79)90095-4).
- Gunnarsson, L.Å.H. and Rönnow, P.H. (1982) Interrelationships between sulfate reducing and methane producing bacteria in coastal sediments with intense sulfide production. *Marine Biology*, 69(2), 121–128. Available at: doi:<https://doi.org/10.1007/BF00396891>.
- Hallam, A., Grose, J.A. and Ruffell, A.H. (1991) Palaeoclimatic significance of changes in clay mineralogy across the Jurassic-Cretaceous boundary in England and France. *Palaeogeography, Palaeoclimatology, Palaeoecology*, 81(3), 173–187. Available at: doi:[https://doi.org/10.1016/0031-0182\(91\)90146-I](https://doi.org/10.1016/0031-0182(91)90146-I).
- Harazim, D. and McIlroy, D. (2015) Mud-rich density-driven flows along an early ordovician storm-dominated shoreline: implications for Shallow-Marine Facies Models. *Journal of Sedimentary Research*, 85(5), 509–528. Available at: doi:<https://doi.org/10.2110/jsr.2015.38>.
- Hein, J.R. and Scholl, D.W. (1978) Diagenesis and distribution of late Cenozoic volcanic sediment in the southern Bering Sea. *Geological Society of America Bulletin*, 89(2), 197–210. Available at: doi:[https://doi.org/10.1130/0016-7606\(1978\)89<197:dadolc>2.0.co;2](https://doi.org/10.1130/0016-7606(1978)89<197:dadolc>2.0.co;2).
- Hillier, S., Matyas, J., Matter, A. and Vasseur, G. (1995) Illite/smectite diagenesis and its variable correlation with vitrinite reflectance. *Clays and Clay Minerals*, 43(2), 174–183.
- Huang, W.-L., Longo, J.M. and Pevear, D.R. (1993) An experimentally derived kinetic model for smectite-to-illite conversion and its use as a geothermometer. *Clays and Clay Minerals*, 41(2), 162–177.
- Junttila, J., Ruikka, M. and Strand, K. (2005) Clay-mineral assemblages in high-resolution Plio-Pleistocene interval at ODP Site 1165, Prydz Bay, Antarctica. *Global and Planetary Change*, 45(1), 151–163. Available at: doi:<https://doi.org/10.1016/j.gloplacha.2004.09.007>.
- Kauffman, E.G. (1977) Geological and biological overview: Western Interior Cretaceous basin. *Mountain Geologist*, 14(3–4), 75–99.

- Kauffman, E.G. (1985). Cretaceous evolution of the Western Interior Basin of the United States. In Pratt, L.M., Kauffman, E.G. and Zelt, F.B. (Eds.), *Fine-Grained Deposits and Biofacies of the Cretaceous Western Interior Seaway: Evidence of Cyclic Sedimentary Processes*. Tulsa, OK: Society of Economic Paleontologists and Mineralogists, Vol. 4, pp. iv-xiii.
- Kauffman, E.G. and Caldwell, W.G.E. (1993). The Western Interior Basin in space and time. In Caldwell, W.G.E. and Kauffman, E.G. (Eds.), *Evolution of the Western Interior Basin*. Canada: Geological Association of Canada. Special Paper 39, pp. 1–30.
- Kemp, S.J., Ellis, M.A., Mounteney, I. and Kender, S. (2016) Palaeoclimatic implications of high-resolution clay mineral assemblages preceding and across the onset of the Palaeocene-Eocene Thermal Maximum, North Sea Basin. *Clay Minerals*, 51(5), 793–813. Available at: doi:<https://doi.org/10.1180/claym.in.2016.051.5.08>.
- Laycock, D.P., Pedersen, P.K., Montgomery, B.C. and Spencer, R.J. (2017) Identification, characterization, and statistical analysis of mudstone aggregate clasts, Cretaceous Carlile Formation, Central Alberta, Canada. *Marine and Petroleum Geology*, 84, 49–63. Available at: doi:<https://doi.org/10.1016/j.marpetgeo.2017.03.012>.
- Lazar, R., Bohacs, K.M., Schieber, J., Macquaker, J. and Demko, T. (2015). *Mudstone Primer: Lithofacies variations, diagnostic criteria, and sedimentologic/stratigraphic implications at lamina to bed-set scale*. SEPM Concepts in Sedimentology and Paleontology #12.
- Leithold, E.L. (1994) Stratigraphical architecture at the muddy margin of the Cretaceous Western Interior Seaway, southern Utah. *Sedimentology*, 41(3), 521–542. Available at: doi:<https://doi.org/10.1111/j.1365-3091.1994.tb02009.x>.
- Leithold, E.L. and Dean, W.E. (1998) Depositional processes and carbon burial on a Turonian prodelta at the margin of the Western Interior Seaway. *Concepts in Sedimentology and Paleontology*, 6, 189–200.
- Li, Z. and Schieber, J. (2018a) Detailed facies analysis of the Upper Cretaceous Tununk Shale Member, Henry Mountains Region, Utah: implications for mudstone depositional models in epicontinental seas. *Sedimentary Geology*, 364, 141–159. Available at: doi:<https://doi.org/10.1016/j.sedgeo.2017.12.015>.
- Li, Z. and Schieber, J. (2018b) Composite Particles in Mudstones: examples from the Late Cretaceous Tununk Shale Member of the Mancos Shale Formation. *Journal of Sedimentary Research*, 88(12), 1319–1344. Available at: doi:<https://doi.org/10.2110/jsr.2018.69>.
- Li, G., Peacock, D.R. and Coombs, D.S. (1997) Transformation of smectite to illite in bentonite and associated sediments from Kaka Point, New Zealand: contrast in rate and mechanism. *Clays and Clay Minerals*, 45(1), 54–67.
- Li, Z., Bhattacharya, J. and Schieber, J. (2015) Evaluating along-strike variation using thin-bedded facies analysis, Upper Cretaceous Ferron Notom Delta, Utah. *Sedimentology*, 62(7), 2060–2089. Available at: doi:<https://doi.org/10.1111/sed.12219>.
- Liu, Z., Colin, C., Li, X., Zhao, Y., Tuo, S., Chen, Z. et al. (2010) Clay mineral distribution in surface sediments of the northeastern South China Sea and surrounding fluvial drainage basins: source and transport. *Marine Geology*, 277(1), 48–60. Available at: doi:<https://doi.org/10.1016/j.margeo.2010.08.010>.
- Livaccari, R.F. (1991) Role of crustal thickening and extensional collapse in the tectonic evolution of the Sevier-Laramide orogeny, western United States. *Geology*, 19(11), 1104–1107. Available at: doi:[https://doi.org/10.1130/0091-7613\(1991\)019<1104:ROCTA>2.3.CO;2](https://doi.org/10.1130/0091-7613(1991)019<1104:ROCTA>2.3.CO;2).
- Lobza, V. and Schieber, J. (1999) Biogenic sedimentary structures produced by worms in soupy, soft muds: observations from the Chattanooga Shale (Upper Devonian) and experiments. *Journal of Sedimentary Research*, 69(5), Available at: doi:<https://doi.org/10.2110/jsr.69.1041>.
- Macaulay, C.I., Haszeldine, R.S. and Fallick, A.E. (1993) Distribution, chemistry, isotopic composition and origin of diagenetic carbonates; Magnus Sandstone, North Sea. *Journal of Sedimentary Research*, 63(1), 33–43. Available at: doi:<https://doi.org/10.1306/D4267A82-2B26-11D7-8648000102C1865D>.
- MacEachern, J.A., Bann, K.L., Bhattacharya, J.P. and Howell, C.D. Jr (2005) Ichnology of deltas: organism responses to the dynamic interplay of rivers, waves, storms, and tides. *SEPM Special Publication*, 83, 49–85.
- Mackenzie, F.T. and Kump, L.R. (1995) Reverse weathering, clay mineral formation, and oceanic element cycles. *Science*, 270(5236), 586–587. Available at: doi:<https://doi.org/10.1126/science.270.5236.586>.
- Macquaker, J.H.S., Keller, M.A. and Davies, S.J. (2010) Algal blooms and “marine snow”: mechanisms that enhance preservation of organic carbon in ancient fine-grained sediments. *Journal of Sedimentary Research*, 80(11), 934–942. Available at: doi:<https://doi.org/10.2110/jsr.2010.085>.
- Macquaker, J.H.S., Taylor, K.G., Keller, M. and Polya, D. (2014) Compositional controls on early diagenetic pathways in fine-grained sedimentary rocks: implications for predicting unconventional reservoir attributes of mudstones. *AAPG Bulletin*, 98(3), 587–603. Available at: doi:<https://doi.org/10.1306/08201311176>.
- Manning, D.A.C., Rae, E.I.C. and Gestsdóttir, K. (1994) Appraisal of the use of experimental and analogue studies in the assessment of the role of organic acid anions in diagenesis. *Marine and Petroleum Geology*, 11(1), 10–19. Available at: doi:[https://doi.org/10.1016/0264-8172\(94\)90004-3](https://doi.org/10.1016/0264-8172(94)90004-3).
- Michalopoulos, P. and Aller, R.C. (1995) Rapid clay mineral formation in Amazon Delta Sediments: reverse weathering and oceanic elemental cycles. *Science*, 270(5236), 614. Available at: doi:<https://doi.org/10.1126/science.270.5236.614>.
- Moncure, G.K., Lahann, R.W. and Siebert, R.M. (1984) Origin of secondary porosity and cement distribution in a sandstone/shale sequence from the Frio Formation (Oligocene). *AAPG Memoir*, 37, 151–161.
- Moore, D.M. and Reynolds, R.C. (1997) *X-ray diffraction and the identification and analysis of clay minerals*. Oxford, England: Oxford University Press.
- Nadeau, P.H. and Reynolds, R.C. (1981a) Burial and contact metamorphism in the Mancos Shale. *Clays and Clay Minerals*, 29(4), 249–259.
- Nadeau, P.H. and Reynolds, R.C. (1981b) Volcanic components in pelitic sediments. *Nature*, 294(5836), 72–74. Available at: doi:<https://doi.org/10.1038/294072a0>.
- Odin, G.S. (1990) Clay mineral formation at the continent-ocean boundary: the verdine facies. *Clay Minerals*, 25(4), 477–483. Available at: doi:<https://doi.org/10.1180/claymin.1990.025.4.06>.
- Perry, E. and Hower, J. (1970) Burial diagenesis in Gulf Coast pelitic sediments. *Clays and Clay Minerals*, 18(3), 165–177.
- Peterson, F., Ryder, R.T. and Law, B.E. (1980) Stratigraphy, sedimentology, and regional relationships of the Cretaceous System in the Henry Mountains region, Utah. *Utah Geological Association Publication*(8), pp. 151–170.

- Plint, A.G., Macquaker, J.H. and Varban, B.L. (2012) Bedload transport of mud across a wide, storm-influenced ramp: Cenomanian-Turonian Kaskapau Formation, Western Canada Foreland Basin. *Journal of Sedimentary Research*, 82(11), 801–822. Available at: doi:<https://doi.org/10.2110/jsr.2012.64>.
- Pollastro, R.M. (1993) Considerations and applications of the illite/smectite geothermometer in hydrocarbon-bearing rocks of Miocene to Mississippian age. *Clays and Clay Minerals*, 41(2), 119–133.
- Pollastro, R.M. and Martinez, C.J. (1985) Whole-rock, insoluble residue, and clay mineralogies of marl, chalk, and bentonite, Smoky Hill Shale Member, Niobrara Formation near Pueblo, Colorado—depositional and diagenetic implications. In: Pratt, L.M., Kauffman, E.G. and Zelt, F.B. (Eds.) *Fine-grained Deposits and Biofacies of the Cretaceous Western Interior Seaway: Evidence of Cyclic Sedimentary Processes*. 4, Tulsa, OK: Society of Economic Paleontologists and Mineralogists, pp. 215–222.
- Potter, P.E., Maynard, J.B. and Depetris, P.J. (2005) *Mud and Mudstones: Introduction and Overview*. Berlin, Heidelberg: Springer-Verlag.
- Pratt, L.M. (1984) Influence of paleoenvironmental factors on preservation of organic matter in Middle Cretaceous Greenhorn Formation, Pueblo, Colorado. *AAPG Bulletin*, 68(9), 1146–1159.
- Price, K.L. and McDowell, S.D. (1993) Illite/smectite geothermometry of the Proterozoic Oronto Group, Midcontinent Rift system. *Clays and Clay Minerals*, 41(2), 134–147.
- Raiswell, R. (1988) Evidence for surface reaction-controlled growth of carbonate concretions in shales. *Sedimentology*, 35(4), 571–575. Available at: doi:<https://doi.org/10.1111/j.1365-3091.1988.tb01236.x>.
- Raiswell, R. and Fisher, Q.J. (2000) Mudrock-hosted carbonate concretions: a review of growth mechanisms and their influence on chemical and isotopic composition. *Journal of the Geological Society*, 157(1), 239–251. Available at: doi:<https://doi.org/10.1144/jgs.157.1.239>.
- Rettke, R.C. (1981) Probable burial diagenetic and provenance effects on Dakota Group clay mineralogy, Denver Basin. *Journal of Sedimentary Research*, 51(2), 541. Available at: doi:<https://doi.org/10.1306/212F7CCF-2B24-11D7-8648000102C1865D>.
- Robert, C. and Kennett, J.P. (1997) Antarctic continental weathering changes during Eocene-Oligocene cryosphere expansion: clay mineral and oxygen isotope evidence. *Geology*, 25(7), 587–590. Available at: doi:[https://doi.org/10.1130/0091-7613\(1997\)025<0587:acwcde>2.3.co;2](https://doi.org/10.1130/0091-7613(1997)025<0587:acwcde>2.3.co;2).
- Ruffell, A., McKinley, J.M. and Worden, R.H. (2002) Comparison of clay mineral stratigraphy to other proxy palaeoclimate indicators in the Mesozoic of NW Europe. *Philosophical Transactions of the Royal Society of London. Series A: Mathematical, Physical and Engineering Sciences*, 360(1793), 675–693. Available at: doi:<https://doi.org/10.1098/rsta.2001.0961>.
- Ryer, T. and Lovekin, J. (1986) The Upper Cretaceous Vernal Delta of Utah—depositional or paleotectonic feature. In: Peterson, J.A. (Ed.) *Paleotectonics and Sedimentation in the Rocky Mountain Region, United States: Part III*. American Association of Petroleum Geologists Memoir, Vol. 41, pp. 497–509.
- Sageman, B.B., Rich, J., Arthur, M.A., Birchfield, G.E. and Dean, W.E. (1997) Evidence for Milankovitch periodicities in Cenomanian-Turonian lithologic and geochemical cycles, Western Interior U.S.A. *Journal of Sedimentary Research*, 67(2), 286–302. Available at: doi:<https://doi.org/10.1306/D4268554-2B26-11D7-8648000102C1865D>.
- Savrda, C.E. and Bottjer, D.J. (1991) Oxygen-related biofacies in marine strata: an overview and update. *Geological Society, London, Special Publications*, 58(1), 201–219. Available at: doi:<https://doi.org/10.1144/gsl.sp.1991.058.01.14>.
- Schamel, S.C. (2008) Potential shale gas resources of Utah. In: Hill, D., Lillis, P. and Curtis, J. (Eds.) *Gas Shale in the Rocky Mountains and Beyond*. Rocky Mountain Association of Geologists, pp. 119–161.
- Schieber, J. (2016a) Mud re-distribution in epicontinental basins—exploring likely processes. *Marine and Petroleum Geology*, 71, 119–133. Available at: doi:<https://doi.org/10.1016/j.marpetgeo.2015.12.014>.
- Schieber, J. (2016b) Experimental testing of the transport-durability of Shale lithics and its implications for interpreting the rock record. *Sedimentary Geology*, 331, 162–169. Available at: doi:<https://doi.org/10.1016/j.sedgeo.2015.11.006>.
- Schieber, J., Lazar, R., Bohacs, K., Klimentidis, R., Dumitrescu, M. and Ottmann, J. (2016). An SEM STUDY OF POROSITY IN the Eagle Ford Shale of Texas—pore types and porosity distribution in a depositional and sequence-stratigraphic context. In Breyer, J. (Ed.), *The Eagle Ford Shale: A Renaissance in U.S. Oil Production*. AAPG Memoir 110, pp. 167–186.
- Schultz, L.G. (1978) *Mixed-layer clay in the Pierre Shale and equivalent rocks, northern Great Plains region (1064A)*. Available at: <http://pubs.er.usgs.gov/publication/pp1064A>
- Sethi, P.S. and Leithold, E.L. (1994) Climatic cyclicity and terrigenous sediment influx to the early Turonian Greenhorn Sea, southern Utah. *Journal of Sedimentary Research*, 64(1b), 26–39. Available at: doi:<https://doi.org/10.1306/D4267F3C-2B26-11D7-8648000102C1865D>.
- Shchepetkina, A., Gingras, M.K. and Pemberton, S.G. (2018) Modern observations of floccule ripples: Petitcodiac River estuary, New Brunswick, Canada. *Sedimentology*, 65(2), 582–596. Available at: doi:<https://doi.org/10.1111/sed.12393>.
- Singer, A. (1980) The paleoclimatic interpretation of clay minerals in soils and weathering profiles. *Earth-Science Reviews*, 15(4), 303–326. Available at: doi:[https://doi.org/10.1016/0012-8252\(80\)90113-0](https://doi.org/10.1016/0012-8252(80)90113-0).
- Singer, A. (1984) The paleoclimatic interpretation of clay minerals in sediments—a review. *Earth-Science Reviews*, 21(4), 251–293. Available at: doi:[https://doi.org/10.1016/0012-8252\(84\)90055-2](https://doi.org/10.1016/0012-8252(84)90055-2).
- Slaughter, M. and Hamil, M. (1970) Model for deposition of volcanic ash and resulting bentonite. *Geological Society of America Bulletin*, 81(3), 961–968. Available at: doi:[https://doi.org/10.1130/0016-7606\(1970\)81\[961:mfdova\]2.0.co;2](https://doi.org/10.1130/0016-7606(1970)81[961:mfdova]2.0.co;2).
- Slingerland, R. and Keen, T.R. (1999). Sediment transport in the Western Interior Seaway of North America: predictions from a climate-ocean-sediment model. In Bergman, K.M. and Snedden, J.W. (Eds.), *Isolated Shallow Marine Sand Bodies*. Tulsa, OK: SEPM Special Publication, Vol. 64, pp. 179–190.
- Środoń, J. (1980) Precise identification of Illite/smectite interstratifications by X-ray powder diffraction. *Clays and Clay Minerals*, 28(6), 401–411. Available at: doi:<https://doi.org/10.1346/CCMN.1980.0280601>.
- Środoń, J. (1981) X-ray identification of randomly interstratified illite-smectite in mixtures with discrete illite. *Clay Minerals*, 16(3), 297–304. Available at: doi:<https://doi.org/10.1180/claymin.1981.016.3.07>.
- Sucha, V., Kraus, I., Gerthofferova, H., Petes, J. and Serekova, M. (1993) Smectite to illite conversion in bentonites and shales of the

- East Slovak Basin. *Clay Minerals*, 28(2), 243–253. Available at: doi:<https://doi.org/10.1180/claymin.1993.028.2.06>.
- Surdam, R.C. and Crossey, L.J. (1985) Organic-inorganic reactions during progressive burial: key to porosity and permeability enhancement and preservation. *Philosophical Transactions of the Royal Society of London*, A315(1531), 135–156. Available at: doi:<https://doi.org/10.1098/rsta.1985.0034>.
- Surdam, R.C., MacGowan, D.B. and Dunn, T.L. (1989) Diagenetic pathways of sandstone and shale sequences. *Rocky Mountain Geology*, 27(1), 21–31.
- Tamburini, F., Adatte, T., Föllmi, K., Bernasconi, S.M. and Steinmann, P. (2003) Investigating the history of East Asian monsoon and climate during the last glacial–interglacial period (0–140 000 years): mineralogy and geochemistry of ODP Sites 1143 and 1144, South China Sea. *Marine Geology*, 201(1), 147–168. Available at: doi:[https://doi.org/10.1016/S0025-3227\(03\)00214-7](https://doi.org/10.1016/S0025-3227(03)00214-7).
- Taylor, K.G. and Macquaker, J.H.S. (2014) Diagenetic alterations in a silt- and clay-rich mudstone succession: an example from the Upper Cretaceous Mancos Shale of Utah, USA. *Clay Minerals*, 49(2), 213–227. Available at: doi:<https://doi.org/10.1180/claymin.2014.049.2.05>.
- Taylor, K.G., Gawthorpe, R.L., Curtis, C.D., Marshall, J.D. and Awwiller, D.N. (2000) Carbonate cementation in a sequence-stratigraphic framework: upper cretaceous sandstones, Book Cliffs, Utah–Colorado. *Journal of Sedimentary Research*, 70(2), 360–372. Available at: doi:<https://doi.org/10.1306/2DC40916-0E47-11D7-8643000102C1865D>.
- Thiry, M. (2000) Palaeoclimatic interpretation of clay minerals in marine deposits: an outlook from the continental origin. *Earth-Science Reviews*, 49(1), 201–221. Available at: doi:[https://doi.org/10.1016/S0012-8252\(99\)00054-9](https://doi.org/10.1016/S0012-8252(99)00054-9).
- Uysal, I.T., Glikson, M., Golding, S.D. and Audsley, F. (2000) The thermal history of the Bowen Basin, Queensland, Australia: vitrinite reflectance and clay mineralogy of Late Permian coal measures. *Tectonophysics*, 323(1), 105–129. Available at: doi:[https://doi.org/10.1016/S0040-1951\(00\)00098-6](https://doi.org/10.1016/S0040-1951(00)00098-6).
- Velde, B. (1995) *Origin and mineralogy of clays, clay and the environment*. Berlin, Heidelberg, Germany: Springer-Verlag.
- Wendler, J.E., Wendler, I., Vogt, C. and Kuss, J. (2016) Link between cyclic eustatic sea-level change and continental weathering: evidence for aquifer-eustasy in the Cretaceous. *Palaeogeography, Palaeoclimatology, Palaeoecology*, 441(Part 3), 430–437. Available at: doi:<https://doi.org/10.1016/j.palaeo.2015.08.014>.
- Wheatcroft, R.A. and Drake, D.E. (2003) Post-depositional alteration and preservation of sedimentary event layers on continental margins, I. The role of episodic sedimentation. *Marine Geology*, 199(1–2), 123–137. Available at: doi:[https://doi.org/10.1016/S0025-3227\(03\)00146-4](https://doi.org/10.1016/S0025-3227(03)00146-4).
- Wilson, R.D. and Schieber, J. (2015) Sedimentary facies and depositional environment of the Middle Devonian Genesee Formation of New York, U.S.A. *Journal of Sedimentary Research*, 85, 1393–1415. Available at: doi:<https://doi.org/10.2110/jsr.2015.88>.
- Wilson, T.R.S., Thomson, J., Colley, S., Hydes, D.J., Higgs, N.C. and Sørensen, J. (1985) Early organic diagenesis: the significance of progressive subsurface oxidation fronts in pelagic sediments. *Geochimica et Cosmochimica Acta*, 49(3), 811–822. Available at: doi:[https://doi.org/10.1016/0016-7037\(85\)90174-7](https://doi.org/10.1016/0016-7037(85)90174-7).
- Xu, G., Deconinck, J.F., Feng, Q., Baudin, F., Pellenard, P., Shen, J. et al. (2017) Clay mineralogical characteristics at the Permian-Triassic Shangsi section and their paleoenvironmental and/or paleoclimatic significance. *Palaeogeography, Palaeoclimatology, Palaeoecology*, 474, 152–163. Available at: doi:<https://doi.org/10.1016/j.palaeo.2016.07.036>.
- Yonkee, W.A. and Weil, A.B. (2015) Tectonic evolution of the Sevier and Laramide belts within the North American Cordillera orogenic system. *Earth-Science Reviews*, 150, 531–593. Available at: doi:<https://doi.org/10.1016/j.earscirev.2015.08.001>.
- Zelt, F.B. (1985) *Natural gamma-ray spectrometry, lithofacies, and depositional environments of selected upper Cretaceous marine mudrocks, western United States, including Tropic Shale and Tununk Member of Mancos Shale*. Princeton, NJ: Princeton University.

How to cite this article: Li Z, Schieber J, Bish D. Decoding the origins and sources of clay minerals in the Upper Cretaceous Tununk Shale of south-central Utah: Implications for the pursuit of climate and burial histories. *Depositional Rec.* 2020;6:172–191.
<https://doi.org/10.1002/dep2.93>